

2006

Comparison of the Variation between ASCE Penman-Monteith Reference Evapotranspiration and Potential Evaporation in Oregon

Chad M. Cary
Portland State University

Follow this and additional works at: https://pdxscholar.library.pdx.edu/open_access_etds

Let us know how access to this document benefits you.

Recommended Citation

Cary, Chad M., "Comparison of the Variation between ASCE Penman-Monteith Reference Evapotranspiration and Potential Evaporation in Oregon" (2006). *Dissertations and Theses*. Paper 6602. <https://doi.org/10.15760/etd.3735>

This Thesis is brought to you for free and open access. It has been accepted for inclusion in Dissertations and Theses by an authorized administrator of PDXScholar. Please contact us if we can make this document more accessible: pdxscholar@pdx.edu.

THESIS APPROVAL

The abstract and thesis of Chad M. Cary for the Master of Science in Geography were presented June 14, 2006, and accepted by the thesis committee and the department.

COMMITTEE APPROVALS:


Daniel Johnson, Chair


Heejun Chang


Geoffrey Duh


Christina Hulbe
Representative of the Office of Graduate Studies

DEPARTMENT APPROVAL:


Martha Works, Chair
Department of Geography

ABSTRACT

An abstract of the thesis of Chad M. Cary for the Master of Science in Geography presented June 14, 2006.

Title: Comparison of the Variation between ASCE Penman-Monteith Reference Evapotranspiration and Potential Evaporation in Oregon

Evapotranspiration (ET) is an important input in terrestrial water balance equations used in modeling streamflow. Good ET estimates are critical to producing reasonable seasonal and annual streamflow predictions. Due to the lack of sufficient instruments to directly measure ET, researchers have developed numerous empirical equations that use climatic variables to estimate this element. Based on studies over the last 50 years, the American Society of Civil Engineers (ASCE) has standardized the calculation of evapotranspiration with the Penman-Monteith equation. Using the ASCE Penman-Monteith equation, this study compares reference ET (ET_0) estimates to potential evaporation (PE) generated from a study completed in 1982 (Farnsworth et al.) and then tests the ET_0 operational performance using a water balance equation. After comparing the two data sets, the 1982 PE estimates showed little variation throughout Oregon relative to the reference ET estimates. In contrast to the 1982 study, data derived from the ASCE Penman-Monteith equations show that there is no relationship between decreasing ET_0 and increasing elevation in Oregon. Despite ET_0 better representing the spatial variation of this element in Oregon, its operational

performance when applied in a water balance model failed to accurately simulate natural evapotranspiration.

COMPARISON OF THE VARIATION BETWEEN ASCE PENMAN-
MONTEITH REFERENCE EVAPOTRANSPIRATION AND POTENTIAL
EVAPORATION IN OREGON

by

CHAD M. CARY

A thesis submitted in partial fulfillment of the
requirements of the degree of

MASTER OF SCIENCE
in
GEOGRAPHY

Portland State University
2006

ACKNOWLEDGEMENTS

From construction to completion the undertaking of this thesis has been an extremely challenging and rewarding experience. Only with the assistance of my committee members, the staff at NOAA's Northwest River Forecast Center and my wife am I able to finish the degree.

My committee members Dr. Johnson, Dr. Chang, Dr. Duh, and Dr. Hulbe showed excellent support and enthusiasm throughout the thesis process. I am very thankful for the effort and time they expended on my ideas, questions, and imagination. My advisor, Dr. Johnson, was the perfect leader for this research endeavor. Under Dr. Johnson, I was able to work independently, yet he was always quick to assist me whenever I needed guidance, motivation, and the truth. I feel fortunate to have been able to work with Dr. Johnson.

The staff at the river center could not have been more accommodating during my pursuit of this degree. Numerous members provided guidance, ideas, critiques and encouragement during almost every challenging aspect of the project. The river center proved their commitment to my completing the degree through flexible scheduling and financial support.

Above all else, my wife, Dayna, has been a tremendous support during the entire process. She has been my sounding board, my best critic, and kept me inspired to the end. I am incredibly grateful to have such an intelligent, caring, and supportive woman in my life.

TABLE OF CONTENTS

ACKNOWLEDGEMENTS.....	i
LIST OF TABLES.....	iv
LIST OF FIGURES.....	v
LIST OF EQUATIONS.....	vi
INTRODUCTION.....	1
BACKGROUND.....	3
Potential Evaporation.....	7
NWRFC and Streamflow Modeling.....	8
STUDY AREA.....	10
METHODOLOGY.....	15
Data Preparation.....	15
Calculate ETo at Points.....	17
Analysis.....	18
Spatial Variation of ET _o	19
Comparison of ET _o with Evaporation Pans.....	21
Water Balance Application.....	24
Sensitivity of the ASCE Penman-Monteith.....	27
RESULTS AND DISCUSSION.....	28
Elevation and ET _o	28
Transects and ET _o	30
Transects and PE.....	33

Comparison between ET_0 and Pans.....34

Completing the Water Balance Equation.....37

Sensitivity of the ASCE Penman-Monteith Equation.....39

SUMMARY AND PROPOSED RESEARCH.....54

REFERENCES.....57

APPENDIX A: ASCE Penman-Monteith Equation.....60

LIST OF TABLES

4.1	Pan Crop Coefficients.....	24
4.2	River Basin Descriptions.....	26
5.1	Pan/ETo Comparison.....	35
5.2	Water Balance Results.....	37

LIST OF FIGURES

3.1	Oregon Topography and RAWS locations.....	12
3.2	1961-1990 Normal Precipitation.....	12
3.3	Hydrographs.....	13
3.4	Agroclimatic Regions.....	14
4.1	Methodology Flow Chart.....	15
5.1	Coastal Region ETo vs. Elevation.....	41
5.2	ETo vs. Elevation below 611 meters.....	42
5.3	ETo vs. Distance from the Pacific Ocean.....	43
5.4	Northern Latitudinal Transect.....	44
5.5	Central Latitudinal Transect.....	45
5.6	Southern Latitudinal Transect.....	46
5.7	Western Longitudinal Transect.....	47
5.8	Central Longitudinal Transect.....	48
5.9	Eastern Longitudinal Transect.....	49
5.10	ASCE Penman-Monteith Interpolated Grids.....	50
5.11	Hargreaves-Samani Interpolated Grids.....	51
5.12	ETo/Pan Comparison.....	52
5.13	Sensitivity Analysis.....	53

LIST OF EQUATIONS

2.1	ASCE Penman-Monteith Equation.....	6
4.1	Dew Point Equation.....	16

INTRODUCTION

Evapotranspiration (ET) is the atmospheric demand for moisture from soils, plants and free water surfaces (Lu et al. 2003), and is a major component in water balance equations used for simulating streamflow or river forecasting. The majority of research in estimating ET has been in areas where water is scarce and agricultural practices are abundant. However, understanding and accounting for this element in non-agricultural regions is equally as important. With growing populations and seasonal variation in available moisture in the Western United States, each year more stress is applied to water resources from hydroelectric projects, agriculture, consumptive uses, navigation, fisheries, and recreation. Implementing the best possible ET data sets in water balance equations can greatly improve hydrometeorological forecast products that provide guidance for those parties responsible for managing water resources.

Evapotranspiration completes the third leg of the water balance triangle that also includes precipitation and runoff. While it is possible to guess at each side of the triangle where data do not exist or are insufficient using only two inputs, the preferred method is to balance the equation with three independent data sources, providing a system of checks and balances on each element. The goal of this study was to calculate reference ET (ET_0), a non-stressed, well watered freely transpiring 0.12 m tall grassy surface (Allen et al. 1998) using the ASCE Penman-Monteith equation and Hargreaves-Samani equation. The ASCE Penman- Monteith equation is the most recommended equation by experts in the field and the differences between it and the

Hargreaves-Samani are well documented making the two equations ideal for this study (ASCE-EWRI 2004). The results are compared to the results of a previous national study done by Farnsworth et al. (1982). The comparison of the two data sets will determine the need to update the Farnsworth et al. (1982) data set or provide modelers confidence in its representation for the state of Oregon.

BACKGROUND

Over the past fifty years, numerous attempts have been made to estimate ET using direct measurements and empirical equations. The need for these data has traditionally been driven by agricultural regions, such as California, where water use is highly regulated due to poor availability (Hargreaves and Allen 2003). Examples of techniques making direct measurements of ET include National Weather Service (NWS) evaporation pans and privately operated lysimeter devices.

The NWS maintains a network of evaporation pan sites designed to directly measure evaporation in its respective environment. The data from pans are referred to as potential evaporation (PE) and represent a freely evaporating shallow body of water (Farnsworth et al. 1982). The data from these sites rely on adjustment coefficients because evaporation pans are affected by their surrounding environments, instrument design, and instrument maintenance (Grismer et al. 2002). Pan coefficients are the ratio of a free water surface evaporation to observed pan evaporation and can vary from 0.64 - 0.88 depending on upwind fetch distance, wind run, heat loss, and relative humidity surrounding the pan (Farnsworth et al. 1982). Free water surface evaporation is derived at a regulated reservoir where the inflow, release, and evaporation of water can be calculated (Farnsworth et al. 1982). Applying the coefficients allows the pan data to better represent a shallow free water surface that is freely transpiring (Farnsworth et al. 1982). Unfortunately, this information is not always available at the pan site and the network of measuring stations is quite sparse (Grismer et al. 2002). In regions where freezing occurs, data from the winter months

are not available because of icing (Grismer et al. 2002). Previous research has shown that PE is most representative of this natural process if averaged over a monthly or seasonal time period (May-October) (Farnsworth et al. 1982).

Another method of directly measuring ET is by means of a lysimeter. A lysimeter is an engineered structure where water that enters and exits the controlled soil and crop can be measured. Meteorological stations supplying adequate data are also available at lysimeter sites, so calculated ET_0 can be verified against measured data. Lysimeters require constant attention and are quite expensive to operate, thus a good spatial network does not exist. Previous studies have managed lysimeters in specific locations where ET is being studied to verify ET_0 calculations using available meteorological inputs (Allen et al. 1989).

Empirical equations have been used to estimate ET in the absence of directly measured data. These equations range in complexity from simple temperature driven equations, such as the Hargreaves-Samani, to combination equations involving several inputs. The chosen equation is usually dependent on the meteorological data available. Various equations incorporating the early work by Penman (1948) and Monteith (1965) have evolved over the last 50 years into the Penman-Monteith equation. Penman (1948) combined the energy balance with the mass transfer method and derived an equation to compute evaporation for an open water surface. Penman's equation required records of sunshine, temperature, humidity, and wind (Allen et al. 1998). Over the years, researchers, including Dr. H.L. Monteith (1965) have extended this equation to cropped surfaces by introducing aerodynamic and surface resistance

factors caused by vegetation (Allen et al. 1998). Numerous versions of the Penman-Monteith and other equations, including a variety of adjustment coefficients, have been used in ET studies over the years causing for inconsistent results from study to study. As these combination equations have evolved over the years, researchers have chosen to calculate ET_0 rather than evaporation for an open water surface and then applying one coefficient. The consensus is that the differences in aerodynamic, vegetation control and radiation characteristics present a difficult challenge in relating ET from free water surfaces to vegetation (Allen et al. 1998). The reference crop accepted world-wide is grass with alfalfa where extensive research is available regarding its aerodynamic and surface characteristics (Allen et al. 1998).

Recently, in an attempt to create some consistency throughout the field, one universal form of the Penman-Monteith was chosen to estimate ET_0 (ASCE-EWRI 2004). A task force was created to determine one universal equation that would best calculate ET_0 in all regions of the world (ASCE-EWRI 2004). In 1998, members of the American Society of Civil Engineers (ASCE) met to determine a standard equation for estimating ET_0 for a standard crop (ASCE-EWRI 2004). While other methods of calculating ET_0 are accepted where data are sparse or limited, the ASCE task force found the ASCE Penman-Monteith equation to be the best estimator of ET_0 , globally (ASCE-EWRI 2004). Applying the ASCE Penman-Monteith equation with success, in a study published in 1989 (Allen et al.), to sites in Australia, Denmark, Zaire, Colorado, Ohio, California, Idaho, and New Jersey, convinced the task force of this equation's accuracy and they recommend its application when estimating ET_0 in any

region. Further research was done by Itenfisu et al. (2003) to support the recommendation of the equation where it proved effective at 49 diverse sites across the United States. The equation is referred to as the ASCE Penman-Monteith equation (Equation 2.1) (ASCE-EWRI 2004).

$$\text{ASCE Penman-Monteith (24hr time steps)}$$

$$ET_o = \frac{0.4808\Delta(R_n - G) + \gamma(900/(T + 273)) u_2(e_s - e_a)}{\Delta + \gamma(1 + 0.34 u_2)}$$

ET_o = Ref ET (mm/d)	R_n = net rad. at crop surface (MJ/m ² d)
T = air temp at 2 meters (C)	u_2 = wind speed at 2 meters (m/s)
G = soil heat flux (MJ/m ² d)	e_s = saturation vapor pressure (kPa)
e_a = actual vapour press. (kPa)	Δ = slope of vapour pressure (kPa/°C)
γ = psychometric constant (kPa/°C)	

Equation 2.1. ASCE Penman-Monteith Equation and description of variables (ASCE-EWRI. 2004).

The ASCE Penman-Monteith equation can be rendered to calculate ET_o based on hourly, daily, or monthly meteorological data. For purposes of this study, daily ET_o was calculated using daily values. Before ET_o can be estimated, numerous side calculations must be completed to derive several of the variables used as input into the ASCE Penman-Monteith equation. These steps and descriptions are available in Appendix A.

Potential Evaporation, 1982

In the late 1970's, the National Weather Service (NWS) tasked a group of researchers to complete a nationwide evaluation of evaporation. The research resulted in a historical and operational data set of PE for the continental United States. Combining NWS class A pans, privately operated pans, and observations from meteorological stations, the group completed the data set in 1982 (Farnsworth et al.). The PE data set used in the study represents the period from 1956-1970. Only 27% of the pans used in the nationwide study had complete period of records for the period of May-October, thus stations were adjust by prorating data from nearby stations with complete records. In Oregon, a combined total of 24 class A pans and meteorological stations comprised the observation network. To convert the pan data to represent the PE of a free water surface, pan coefficients were applied. For locations in mountainous areas, such as Western States and the Appalachian area of the Eastern United States, USGS maps with the scale of 1:500,000 were used to provide detailed topographic information. In California and New Mexico, the research team discovered that PE decreases with regard to elevation. This relationship was applied to all of the Western United States when isopleths were drawn between valley locations and mountainous areas. Now, 24 years later, this data set is still used operationally in numerous NWS applications.

(Farnsworth et al. 1982)

NWRFC and Streamflow modeling

An operational platform that specializes in simulating streamflow, the Northwest River Forecast Center (NWRFC) relies heavily upon data such as ET to perform its mission. One of 13 national River Forecast Centers, The NWRFC produces short term streamflow forecasts using six hour synoptic interval and long term water supply forecasts predicting volumes up to nine months. The NWRFC jurisdiction extends across seven states in the Pacific Northwest and includes a portion of Southern British Columbia. The operations of the NWRFC require a firm understanding of a variety of weather patterns and climate trends from basin to basin. It is not uncommon for one region of the NWRFC jurisdiction to experience drought like conditions while another is experiencing floods. Accurate accounting for all of the physical conditions occurring across the region enables the NWRFC to better simulate streamflow.

In order for the NWRFC forecasts to effectively simulate streamflow, the water budget of a basin must be balanced. The water budget usually consists of a water balance equation comprised of runoff, precipitation and ET where the equation is: $\text{Runoff} = \text{Precipitation} - \text{ET}$. This equation assumes a closed basin and excludes factors affecting runoff such as percolation and ground water recharge. Before simulating streamflow at a point along any river, the upstream watershed contributing runoff must be calibrated. Basin calibrations rely on historical streamflow, precipitation, temperature, and evapotranspiration data (Anderson 2000). Temperature is used for typing precipitation as either rain or snow. Unfortunately,

direct measurements of precipitation and ET within the delimited boundary of each basin are not always available. In basins where data are unavailable, precipitation and ET are represented by estimates resulting from interpolation methods using surrounding stations. While the results of these interpolations provide data for calibrations where it does not otherwise exist, the estimates are subject to errors and often rely on one another when determining the water balance equation, thus violating the integrity of its purpose.

Currently, NWRFC calibrations use PE data from the study by Farnsworth et al. (1982). The majority of the sites used to estimate PE are from valley locations or foothills. Large scale assumptions, such as a decrease in ET_0 with elevation in areas where there is mountainous topography, were applied to 11 Western States based on findings in two Southwestern States. Large scale assumptions, lack of topographic representation, and age of the study triggered the interest to revisit the dataset.

The objective of this study was to calculate ET_0 using the ASCE Penman-Monteith equation and compare the results to the PE data set generated in 1982. The denser ET_0 data set should indicate where PE lacks representation in Oregon. After analyzing the differences in spatial variability between the two data sets, ET_0 data are used in a water balance equation to test its operational performance. This comparison will determine if the PE data set from 1982 is consistent with the highly regarded ASCE Penman-Monteith equation and if the NWRFC needs to update ET data throughout its jurisdiction.

STUDY AREA

The state of Oregon was chosen as the study area because of its location within the NWRFC jurisdiction and its diverse climate predominantly influenced by mountainous terrain and storm systems originating in the Pacific Ocean (Figure 3.1). Serving as a climate barrier, the Cascade Mountains extend in a north-south orientation and divide the moist western region from the arid eastern region, drawing moisture out of the atmosphere when systems pass through the region (Figure 3.2). As a result, there are two hydrologic regimes in Oregon (Figure 3.3). Hydrographs west of the Cascades experience numerous peaks during the winter months due to isolated heavy precipitation events. Streams draining the west side of the Cascade Range also experience rises in the spring months as the snow pack melts. East of the cascades there is one dominant peak that occurs each spring that is subject winter snow accumulation and seasonal temperature changes (Beebee and Manga 2004).

An example of the stark contrast in climate on opposite sides of the Cascade Crest is evident in the cities Astoria and Baker City. These two cities represent opposite sides of the state with Astoria on the Oregon Coast and Baker City in Eastern Oregon, approximately 560 km inland. Residents of Astoria can expect an average of 173 centimeters of precipitation annually while residents of Baker City rely upon 49 centimeters. Despite climate differences on each side of the Cascade Crest, both regions share a common demand for water resources to fulfill needs by such interests as agriculture, fisheries, hydroelectric generation, navigation, and recreation. The

ability to accurately account for gains and losses in the hydrologic budget of either region are critical.

Oregon's wide range in climate requires the state to be divided up into six agroclimatic regions (Figure 3.4) for the purpose of this study. The six regions are Coastal and Lower Columbia, Willamette Valley, Southwestern Oregon, Columbia Basin, South Central Oregon, and Snake River Basin (Redmond 1985). These divisions are based on general climate characteristics and the complex terrain of Oregon. Dividing the state allows for characteristics associated with ET_o to be isolated, and is recommended from previous research (Martinez-Cob and Cuenca 1991).

Oregon is also an ideal study area to calculate ET_o because of data availability. There are 113 Remote Automated Weather Stations (RAWS) collecting almost all of the elements necessary to calculate ET_o using the ASCE Penman-Monteith equation (Figure 3.1). The RAWS network, funded jointly by the U.S. Forest Service and the National Weather Service, contains sites at a variety of elevations that allows for more diverse representation of measured meteorological data to use as input into the ASCE Penman-Monteith equation. The RAWS network is ideal for this study because it provides almost the entire suite of data necessary to calculate ET_o using the ASCE Penman-Monteith and it provides estimates at a wide range of elevations throughout Oregon.

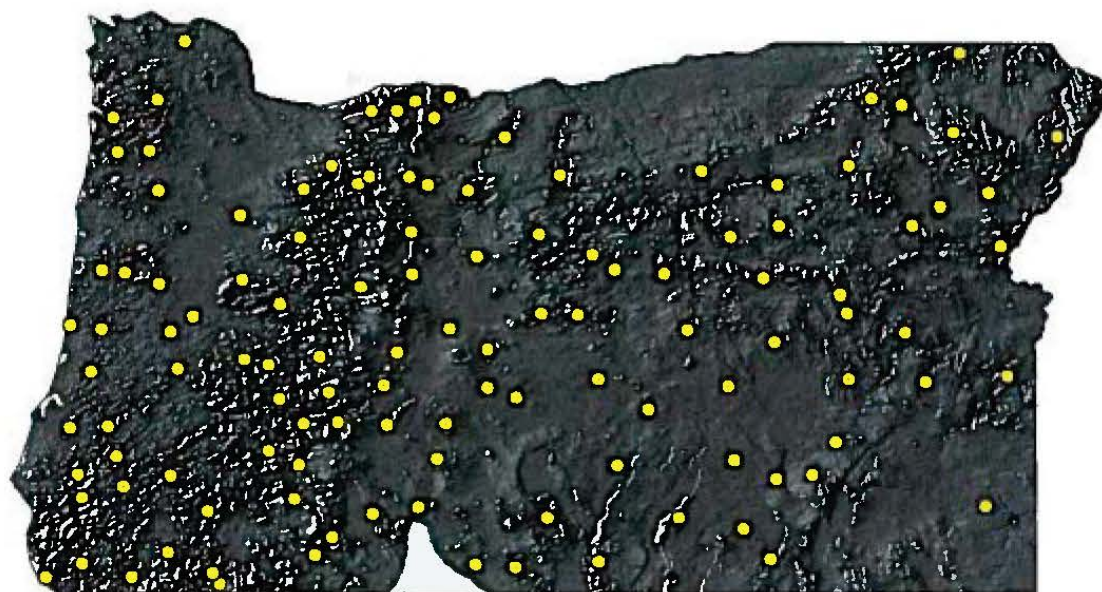


Figure 3.1. Hillshade of Oregon portraying diverse topography and RAWS observation locations.

**Average Annual Precipitation
Oregon**



Period: 1961-1990

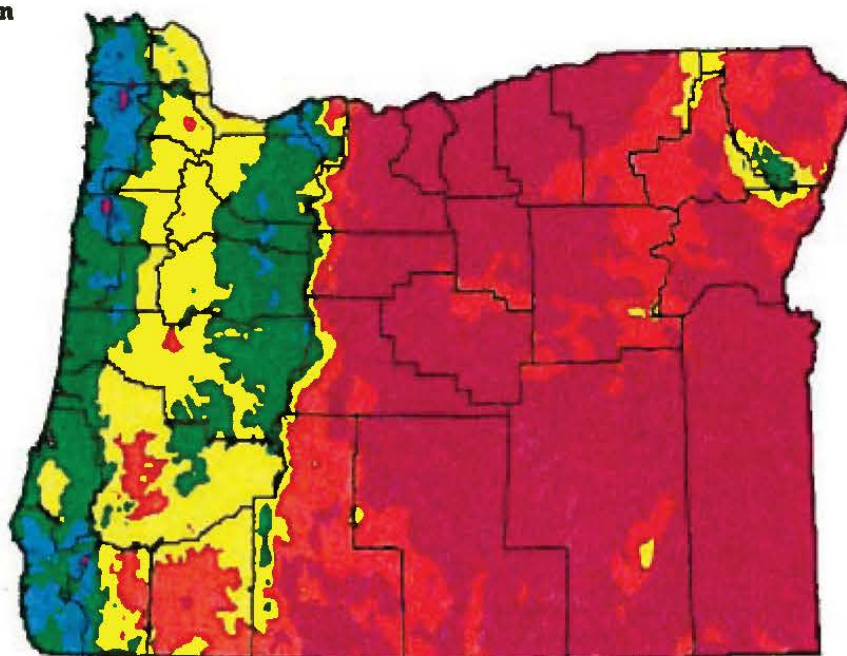
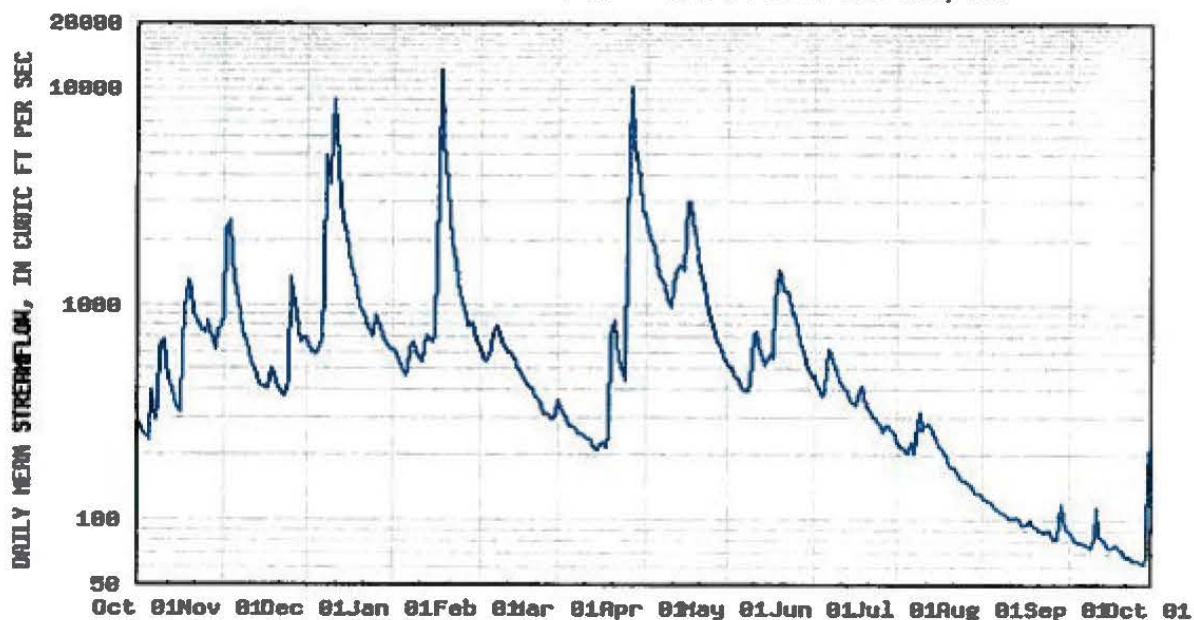


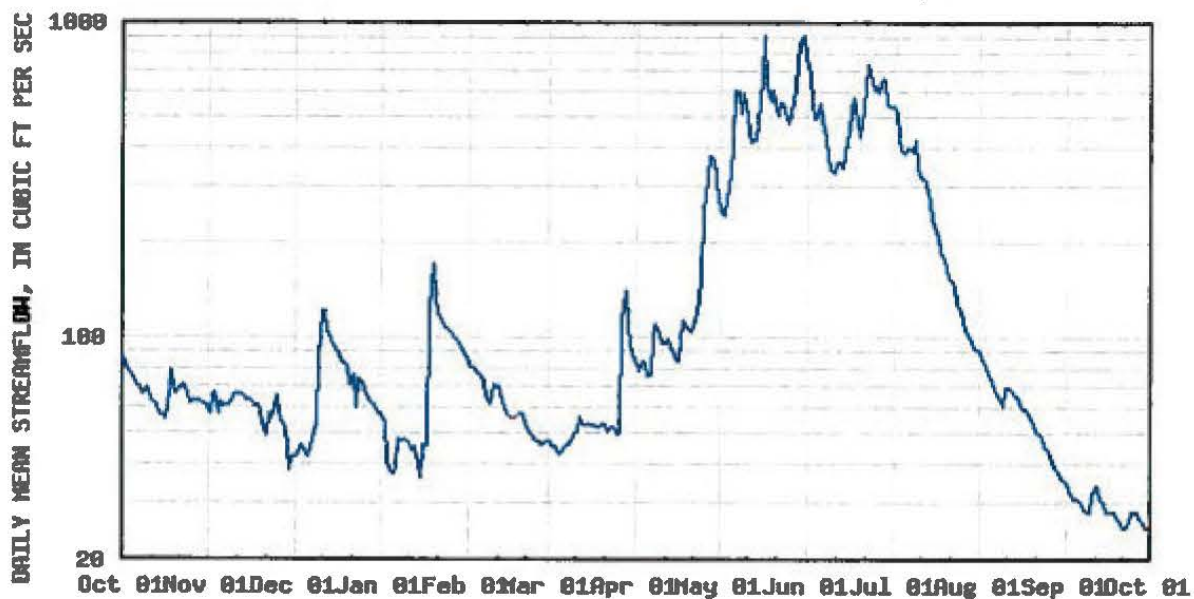
Figure 3.2. 1961-1990 Normal precipitation map of Oregon (Western Region Climate Center May 31, 2006).



USGS 14301500 WILSON RIVER NEAR TILLAMOOK, OR



USGS 13330000 LOSTINE RIVER NEAR LOSTINE, OR



EXPLANATION
 — DAILY MEAN STREAMFLOW — ESTIMATED STREAMFLOW

Figure 3.3. Hydrographs portraying streamflow patterns west (above) of the Cascade Crest and east (below) the Cascade Crest. The western basin is the Wilson River Basin and Eastern Oregon is represented by the Lostine River Basin. (USGS 2006)

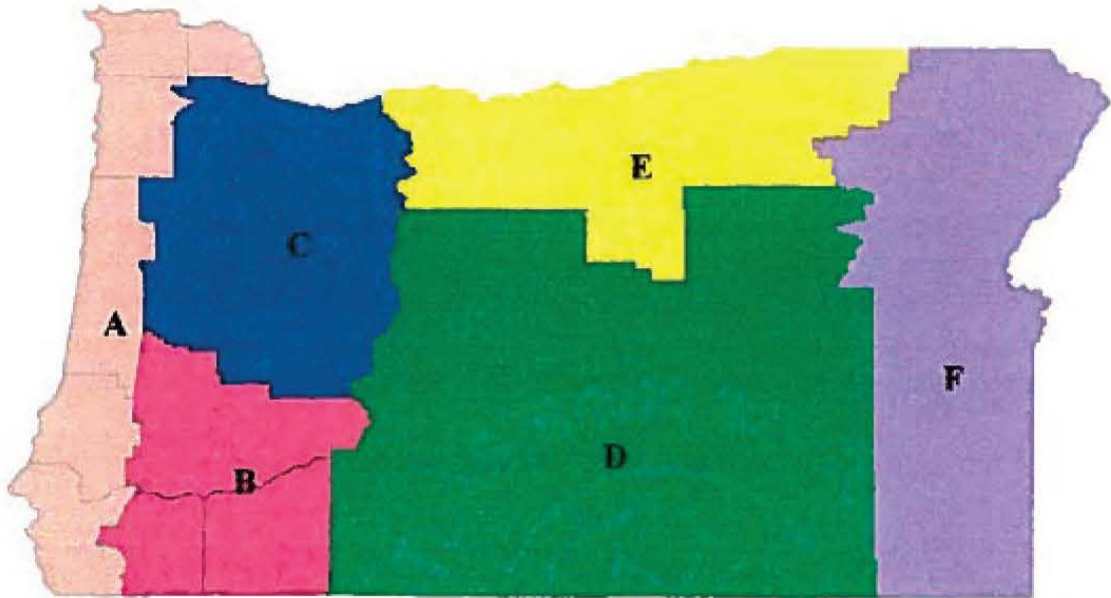


Figure 3.4. Six agroclimatic regions of Oregon: (A) Coastal and Lower Columbia, (B) Southwest Oregon, (C) Willamette Valley, (D) South Central Oregon, (E) Columbia Basin, and (F) Snake Basin.

METHODOLOGY

Reference evapotranspiration was calculated at 113 points in the state of Oregon from 1998-2002. Several steps were required before the spatial data set of ET_o was completed. The flow chart below (Figure 4.1) outlines the sequential steps conducted to complete the project. Several of the methods were executed to confirm findings and methodology from the 1982 (Farnsworth et al.) study and to determine if the spatial variation is consistent between the two data sets.

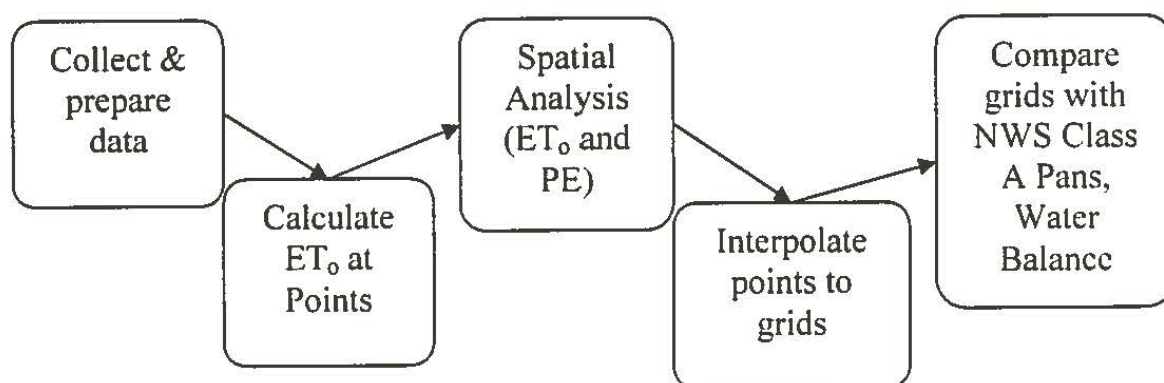


Figure 4.1. Flow chart of study design

Data and Preparation

Beginning in 1985, the RAWS records span 20 years at the oldest stations. The Western Region Climate Center archives daily RAWS data and has thus made it possible to use this resource for gathering maximum and minimum temperature, maximum and minimum relative humidity, average wind, elevation, and geographic position for the period of record. Unfortunately, the RAWS sites do not record dew point and only recently began collecting solar radiation; thus these elements needed to be acquired elsewhere.

The Solar Radiation Monitoring Laboratory at the University of Oregon generates solar radiation grids using satellite derived solar radiation. The solar radiation data base includes 5 years (1998-2002) of daily global solar radiation in 0.1° by 0.1° grids for the Pacific Northwest. The grids were verified using ground observation sites that measure solar radiation in Oregon (Vignola and Perez 2004). The grid cell that geographically encompassed each RAWS was assigned to the respective stations. This data set supplements the missing solar radiation from the RAWS network. Because of the solar radiation data set, the period of analysis in this study spans from 1998-2002. Satellite derived solar radiation is recommended for use in combination equations calculating evaporation (Lindsey and Farnsworth 1997). While other data sets with longer period of records were available, the recommended satellite data set was chosen for use in this study. Once the RAWS data and solar radiation were organized and prepared for the calculations, the last task was to compute dew point using temperature and relative humidity as inputs (Equation 4.1). Dew point is a function of relative humidity and temperature thus these two elements were used as input into the equation below:

$$DP = T - ((14.55 + 0.114T)X + [(2.5 + 0.007T)X]^3 + (15.9 + 0.117T)X^{14})$$

Equation 4.1. Dew point calculation (Linsley et al. 1982)

In the dew point equation (Equation 4.1), T represents max temperature in °C and X represents relative humidity as a percentage. This method estimates dew point to within 0.3° C (Linsley et al. 1982). Calculating dew point completes the data set required to calculate ET_o via the ASCE Penman-Monteith equation.

Calculate ET_o at Points

Once the data set was organized and prepared for computation in the ASCE Penman-Monteith Equation, the next step was to calculate daily ET_o at each RAWS in Oregon. Meteorological inputs into the daily version of the equation (Equation 2.1) are solar radiation, maximum temperature, minimum temperature, mean wind speed, maximum humidity, minimum humidity, elevation, latitude, and mean dew point.

The program used to calculate ET_o was created by Dr. R.L. Snyder from the University of California at Davis. Using the meteorological inputs, the program calculates each of the variables in the ASCE Penman-Monteith equation that are required to compute ET_o . The program is designed to calculate ET_o for a freely transpiring grassy surface 0.12 meter tall and calculates ET_o using the temperature driven Hargreaves-Samani equation (appendix A). The Hargreaves-Samani equation is a valuable tool for checking results for consistency as it only uses maximum temperature, minimum temperature and latitude. Previous research has documented the expected errors when comparing the results of Hargreaves-Samani equations with the ASCE Penman-Monteith results (Allen et al. 1989, Itenfisu et al. 2003, Allen et al. 1998).

Average daily ET_0 values per month are then organized into total monthly, seasonal, and annual temporal resolutions for the five year period. The seasonal period represents May-October, which is an approximation of the growing season in Oregon and is the best period of record for evaporation pans. The result is a spatial data set of ET_0 from 1998-2002. Previous research recommends applying the data in monthly and seasonal resolutions to reduce errors and limit anomalous values from skewing results (Allen et al. 1989). At RAWs, where there are fewer than five days available per month in the time series, the month is discarded. Each station was required to have at least four of the five months to calculate the five year average. Graphical tools imbedded in Dr. Snyder's program plot each type of input and output data. These graphs, plotting daily and monthly values, were used to subjectively scan for outlying numbers that might cause erroneous results.

Analysis

The purpose of the analysis was to determine if the PE data is consistent with the ASCE Penman-Monteith and Hargreaves-Samani calculated ET_0 data and if the ET_0 data set can be applied operationally at the NWRFC. The data used to generate ET_0 is a much higher resolution compared to the PE data and it was presumed that the results will better represent Oregon's diverse climate. The analysis investigated the influence of elevation on regional ET_0 and if this influence is consistent with results from the Farnsworth et al. study (1982). The analysis also examines the spatial differences between PE and ET with regard to distance from the Pacific Ocean and

latitude. After comparing the two data sets, the study will determine if the ET_o data are an effective input into a water balance equation. Because very little research has been done to quantify the spatial characteristics of ET_o in Oregon, an exhaustive search for spatial variations and patterns was required.

Spatial Variation of ET_o

Remote Automated Weather Sites (RAWS) were established in Oregon to measure weather data in forests to assist fire-weather programs that provide weather forecasts during uncontrolled and prescribed burns and to better map the weather in the United States. As a result of these interests, RAWS are located in higher elevations relative to other National Weather Service meteorological observation networks. The average elevation for stations in Oregon with the period of record from 1998-2002 used in this study is 1163 meters, where stations range from 6 to 2021 meters.

Farnsworth et al. (1982), found that PE declined with elevation in California and New Mexico during the growing season (May-October). Using an elevation range from 30–2775 meters in California and 1463-3293 meters in New Mexico, the square of the correlation coefficient (r^2) between elevation and PE was 0.99 (Farnsworth et al. 1982). While this relationship occurs in a different geographic region, the mountainous topography is similar in Oregon and the effect of elevation is worth exploring. Dividing Oregon into six major agroclimatic sub-regions (Redmond 1985), the ET_o data were plotted against elevation and then further isolated with slope aspect.

If a relationship had been found, it would have dictated the interpolation technique used to calculate a raster for Oregon.

Another relationship of interest in this study is how ET_0 and PE change with regard to distance from the Pacific Ocean. Most weather systems that influence the climate in Oregon originate from the Pacific Ocean. To quantify this relationship, two approaches were attempted in this study. The first approach was to plot all of the RAWS in Oregon against their distance from the Pacific Ocean. The results from this plot indicated that there is a trend in the data (Figure 5.3). Once this trend was established, the second approach took three westerly transect lines of RAWS, selected to cover the southern, central, and northern geography of the state. In order to compare PE values at the same geographic location as the RAWS points, the PE grid file was used. Values from a PE grid cell where it encompassed a point were assigned to each RAWS. From this analysis, it became evident how ET_0 changes with regard to distance from the Pacific Ocean.

Another question was how ET_0 and PE change from south to north. This relationship was investigated by drawing three south to north transects in Western, Central, and Eastern Oregon. These three transect lines represent the Coastal Mountain Range, Eastern foothills of the Cascade Mountain Range, and the desert plains of Eastern Oregon. The transect lines investigate how PE varies relative to ET_0 from south to north in three different sections of Oregon.

Comparison of ET_o with Evaporation Pans

Evaporation pans are currently the best available network that directly measures evaporation in Oregon. Evaporation pan data exist for the period of interest from 1998-2002 consistently during the months May-October at 11 locations in Oregon. Two more stations, Klamath Falls and Bend 7NE were also used during the monthly analysis, but neither site had sufficient data during the month of October. While there are several problems with evaporation pan data, these problems are known and the relationship between pan and estimated ET_o is well researched. In arid or windy regions pans tend to overestimate evaporation as much as 20% while in areas with higher relative humidity and cooler temperatures as much as 5-10% (Allen et al. 1998). These adjustments are made using a pan coefficient. Pan coefficients, for this study, are needed for two reasons. The first reason is to compensate for the wind, vegetation, and relative humidity affecting the environment surrounding the pan. The second reason to use the coefficient is to convert the pan data to ET_o . Once the pan coefficient has been applied, the pan data is ready to be compared to the ASCE Penman-Monteith and Hargreaves-Samani calculated ET_o .

Unfortunately, evaporation pans are not co-located with RAWS points. To compare the two data sets, a gridded field of ET_o was generated using inverse-distance-weighting (IDW) and kriging interpolation methods in a GIS (Figures 5.10, 5.11). Where the grid cells encompass the evaporation pan sites, monthly and growing season values for ET_o were extracted. Previous studies (Farnsworth and Thompson 1984) recommend using monthly or seasonal temporal resolutions when

using evaporation pan data to filter the data for erroneous measurements. Plotting the ET_0 and the evaporation pan data against each other portrays the similarity between the two data sets.

The next challenge associated with comparing the ET_0 estimates to pan data as a means of verification is converting pan data to ET_0 using pan coefficients published in the ASCE Penman-Monteith final report (ASCE-EWRI 2004). Converting the pan data to represent ET_0 is necessary so the data are in the same format for effective comparison of the results. Monthly values from May to October and one seasonal value representing the sum from May-October were compared due to evaporation pan limitations during winter months. (Pan data do not exist during winter months in regions where the temperature drops below zero degrees Celsius)

Two interpolation techniques, Inverse Distance Weighting (IDW) and Kriging were chosen because of their simplistic design and availability in a GIS. There is flexibility for choosing an interpolation technique because no significant trends were found between elevation and ET_0 , there is flexibility for choosing an interpolation technique. Each technique uses the nearest six neighboring stations to generate grids of approximately 1 km resolution. Inverse Distance Weighting is a deterministic interpolation method that generates grid cell values using point values. The weight given to each point is a function of inverse distance. Kriging is a statistical method of interpolating points to grids. Kriging, like IDW, assigns weights to neighboring points. However, weights from the kriging technique come from a semivariogram developed by viewing the spatial structure of the data. A semivariogram quantifies the

assumption that neighboring stations tend to be more alike than those farther apart.

To create a continuous surface of ET_0 , predictions are made for grid cells based on the semivariogram and the spatial arrangement of calculated ET_0 values that are nearby.

The grid cell that encompasses the pan station is then used for the comparison made here.

The coefficient used to convert the pan data to ET_0 requires local information on the land cover surrounding the pan, relative humidity, and wind. The meteorological information varies monthly, requiring monthly data from May-October. Such data were collected from the National Climatic Data Center, Bureau of Reclamation's Agrimet archives, Western Region Climate Center's Archives, and Oregon State University's Spatial Climate Analysis Service, and the National Weather Services Cooperative Observers Network. Once the land cover surrounding the pan, wind, and relative humidity were identified, then the proper coefficient could be applied to convert raw pan data to ET_0 for each month.

Pan Station	Crop Coefficient
Wickiup Dam	0.73
North Willamette Exp. Station	0.73
Moro	0.74
Medford Exp. Station	0.75
Lookout Point Dam	0.73
Klamath Falls Agric. Station	0.74
Hood River Exp. Station	0.71
Fern Ridge Dam	0.74
Corvallis State University	0.74
Madras	0.73
Bend 7 NE	0.73
Malhuer Branch	0.70
Pendleton Branch Exp.	0.71
Summer Lake	0.71

Table 4.1. Pan stations and their coefficients used to convert evaporation pan data to the reference grass surface: ET_0 .

Water Balance Application

The ultimate goal of the study was to develop a data set of actual ET that can be applied in basin calibrations. Unfortunately, a complete data set of actual ET

requires a thorough understanding of all water stressed and non-stressed land covers. It also requires abundant information regarding growing seasons, stages of leaves, and other vegetative properties. Summarizing the complexity of these variables into one number, crop coefficients are available for some of these land covers to convert ET_0 to actual ET (ET_a). Using a crop coefficient for evergreen land covers, a type of vegetation that changes very little throughout the calendar year, the study converted ET_0 to ET_a . Four basins were chosen for this analysis in Oregon. Precipitation data from PRISM and runoff data from the United States Geological survey were used to compare the results.

Conceptual hydrologic models require realistic and consistent estimates of evaporation and precipitation in order to produce a proper water balance. While precipitation has its largest effect during individual storms, evapotranspiration estimates are critical to producing good annual and seasonal estimates of the water balance. Biased estimates of evapotranspiration could result in unrealistic streamflow simulations, particularly in dry regions. Before ET_0 can be implemented into a water balance equation, the estimates must be converted to actual ET (ET_a). The evergreen crop coefficient (Snyder et al. 2002) and basins where the predominant land cover is evergreen forest were used to complete a water balance equation. The precipitation and runoff data used to compare the results were from the Spatial Climate Analysis Service where PRISM is generated, and the United States Geological Survey, respectively. Monthly data were used to generate annual means for the period 1998-2002. An annual resolution is necessary because each river basin accumulates snow

during the winter months. Subtracting calendar year runoff from precipitation will give us ET_a that can be compared against calculated ET_a using the equations.

The four basins used exist in different agroclimatic regions and were chosen because of their land cover, importance to the NWRFC, data availability, limited diversions or regulation, and spatial representation (Table 5.2). The land cover data are from the GAP Analysis Program, a project of the Idaho Cooperative Fish and Wildlife Research Unit in cooperation with the Oregon department of Fish and Wildlife (Kagan and Caicco 1996). The images represent 1991.

Basin	NWS ID	Area (ki ²)	Agroclimatic Region	Tributary
Quartzville Creek near Cascadia, OR	qcco3	257	Willamette	Santiam River
Illinois River near Kerby, OR	krbo3	984.2	SW Oregon	Rogue River
Wilson River near Tillamook, OR	tlmo3	417	Coastal	Wilson River
Lostine River near Lostine, OR	lsto3	183.6	Snake River	Wallowa River

Table 4.2. River basins in Oregon used for water balance analysis.

In basin calibrations, the difference between ET and precipitation estimates simulate streamflow in a closed basin. Because streamflow data (runoff) and gridded precipitation data are currently available, the difference between the two serves as a tool to verify basin ET_a . In a GIS, interpolated grids similar to those used during the pan evaporation comparison were used to estimate average ET_o in each basin. Results from the Hargreaves-Samani and ASCE Penman-Monteith equation and both interpolation techniques are used in this analysis for a total of four possible combinations. Annual precipitation estimates for each basin were also acquired using

PRISM precipitation grids. Average monthly streamflow was converted to monthly runoff and then annual runoff for each year from 1998-2002 before being converted to annual runoff. Runoff is a volume that can be compared to precipitation and ET.

Sensitivity of the ASCE Penman-Monteith

A sensitivity analysis of the ASCE Penman-Monteith was conducted to determine how changes to the input parameters impact the ET_0 estimates. The sensitivity analysis is important as it quantifies the effect of a bias in the data set (Frei et al. 2002). One year from one station was chosen as the benchmark value for ET_0 . The methodology for this analysis was to take one year with its original inputs and use the calculated ET_0 data as the baseline or zero values. The next step was to adjust each individual parameter. Because individual parameter values are unique the annual range of variation was derived. Next, using this value the daily data was adjusted by adding 10% during one trial and -10% during the subsequent. This demonstrates the effect of a 10% bias unique to the values of each parameter. Only changing one input per trial and comparing the difference in ET_0 to the baseline values isolates the impact of individual parameters.

RESULTS AND DISCUSSION

Elevation and ET_o

Precipitation amounts are known to increase up to a certain elevation with the combination of slope orientation and elevation; this is known as the orographic influence of topography (Daly et al. 1993). Temperature lapse rates characterize the change in temperature with elevation (Linsley et al. 1982). In general, temperature decreases an average of 0.7° C per 100 meters in the lower troposphere (Linsley et al. 1982). A study conducted by Lu et al. (2003) where actual ET was calculated in Southwestern U.S. also found elevation to be one of the most important environmental elements in the spatial variability of regional ET. In New Mexico and California, Farnsworth et al. (1982) found a highly correlated inverse relationship between PE and elevation. The study also states that above a threshold elevation, depending on the area, there is little or no further decrease of ET_o with elevation.

Surprisingly, in this study, the ET_o data derived from RAWS data input into the ASCE Penman-Monteith and Hargreaves-Samani equations did not show a consistent decrease with elevation change. Throughout each of the six agroclimatic regions, there is no consistent relationship between elevation and ET_o on monthly, seasonal, or annual time periods. In the coastal region ET_o increases with elevation during June, July and August (JJA), with a correlation coefficient of 0.522 (Figure 5.1). The relationship is also apparent during the May-October period with a correlation coefficient of 0.444 (Figure 5.1). These correlation coefficients show a

low correlation. Other agroclimatic regions failed to show any sort of relationship between ET_o and elevation change.

To further isolate the characteristics of topography and elevation, each of the agroclimatic regions were divided up by stations with northern and southern aspect. Northern and Southern aspect stations experience different weather depending on several variables. In general, topography with a Southern aspect at higher elevation receives more daylight hours throughout the year and, on average, receives more precipitation than northerly aspects (Daly et al. 1993). With RAWS sites grouped into the six agroclimatic regions and then by aspect, there was still no apparent relationship between elevation and change in ET_o . If there is a relationship between elevation and actual evapotranspiration, it is most likely driven by different land cover types or perhaps exists below the average height of the RAWS network.

Few stations exist at lower elevations in the RAWS observation network. In the Willamette Valley climate region there are six stations 610 meters and below in elevation that show an inverse relationship between ET_o and elevation when isolated from the surrounding stations (Figure 5.2). Above the 610 meter elevation, the data follow no particular pattern with regard to elevation. This trend was also seen in the Southwestern Oregon region. In this region there is a negative trend between ET_o and elevation with a correlation coefficient of 0.91 below 610 meters. Unfortunately, this sample of three stations is too small thus the results are inconclusive.

Transects and ET_o

Transects were designated to investigate the change of ET_o with regard to latitude and distance from the Pacific Ocean. Many physical and environmental characteristics change with regard to these two independent variables. Traveling north from the southern border of Oregon, temperature and solar radiation decrease. When traveling east from the Pacific Ocean, there is less available moisture in the atmosphere and the conditions become more arid, especially east of the Cascade Crest. These features of Oregon's climate are presumed to have an impact on the spatial variation of ET_o .

When plotting all of the RAWS against their distance from the Pacific Ocean there is a definitive increasing trend in monthly ET_o (Figure 5.3). July has the highest r^2 value at 0.516, with June and August just slightly lower at 0.433 and 0.503 respectively. Another method of analyzing this relationship is to evaluate three latitudinal transect lines of data across Northern, Central, and Southern Oregon. The purpose of these transects was to sample the change in ET_o with regard to distance from the Pacific Ocean. Logarithmic trend-lines are used on these plots to capture when the change in ET_o caused by distance from the Pacific Ocean appears to be unrelated.

The northern transect show an increasing trend in ET_o as distance from the Pacific Ocean increases. This is portrayed in monthly, seasonal and annual temporal resolution in Figure 5.4. Consistent with the previous analysis, the winter months show no trend in this transect or any other transect lines most likely due to the little

correlation coefficients range from 0.50 – 0.66. From May-October, representing the general growing season for the state, the correlation coefficient is 0.65.

The central latitudinal transect lines also show an increasing trend in ET_o further inland (Figure 5.5). During the summer months the correlation coefficients describing the increase in ET_o with linear distance from the Pacific Ocean are 0.66, 0.63, and 0.56, respectively. Along this transect, there is an abrupt increase in ET_o just east of the Cascade Crest in the South-central Agroclimatic region shown in all temporal resolutions. This could be a result of the transition between climate zones and the effects of the rain shadow caused by the Cascade Mountains.

The southern latitudinal transect does not show an increasing trend between ET_o as distance from the Pacific Ocean increases. The RAWS in Southwestern Oregon have higher average ET_o rates per month than do other stations West of the Cascades from south to north. The period from May-October (Figure 5.6) represents the general trend between ET_o and distance from the Pacific on this transect.

In Southwestern Oregon, the data in the valley between the Coast Range and the Cascades is greater than those stations in the same valley located further north during all months. Thus, the transect across Southern Oregon are erratic from west to east and show no trend. Only the data in the Snake Region and Coastal region show a clear trend.

The northern and central latitudinal transects show fairly high correlation between distance from the Pacific Ocean and increasing ET_o using a logarithmic trend line. There was also a distinct change apparent along both transects at the

approximate distance when the change in ET_o seems to become more random.

Approximately 230 kilometers inland, the trend line flattens and changes in ET_o are more likely due to local conditions rather than the temperate maritime influence.

Similar to latitudinal transects, longitudinal transects sample the spatial patterns of ET_o with respect to latitude and distance inland, a span ranging between 410 and 475 km inland. By dissecting the state with three transects running south to north, Western Oregon, Central Oregon, and Eastern Oregon, ET_o characteristics are represented.

The Western Oregon longitudinal transect, which varies between 40 and 100 km inland, resulted in high correlation coefficients representing a decrease in ET_o with an increase in latitude. Unique to these transects are the highly correlated values during the winter months (Figure 5.7). While there is very little ET occurring during winter months (Farnsworth et al. 1982), there is an obvious decrease in ET_o to the north along this transect which is consistent with temperature and solar radiation. The remaining seasonal and annual plots in Figure 5.7 show r^2 values indicating the relationship between decreasing ET_o and increasing latitude in this region of Oregon.

In Central Oregon, the longitudinal transect does not display a clear relationship from south to north. The plot in Figure 5.8 represents ET_o from May-October and displays the correlation. Latitude and ET_o did not show any sort of correlation in this section of the state. The Cascade Mountain Range was probably the cause for this discontinuity in results. There is a stark contrast in climate between the

west side of the Cascade Mountains and the east side and this data exists in the transition zone between these two climate regimes.

Approximately, 560 km inland, the Eastern Oregon longitudinal transect portrays a strong relationship between ET_o and latitude along the Eastern Oregon transect (figure 5.9). During the growing season, the $r^2 = 0.77$. Similar to the Western transect, there was also a strong relationship during the winter months where December, for example, has an r^2 value of 0.73. The data from the remaining months show r^2 values from 0.69 – 0.85 indicating a strong correlation between ET_o and latitude in the Eastern region of Oregon.

Transects and PE

Potential evaporation, compiled in 1982 (Farnsworth et al.) for the continental U.S. is the potential water available to evaporate and is similar to a grassy surface. In comparing the two data sets, the magnitudes are not of interest as they are from different historical time periods, but rather the spatial patterns are compared. The PE data were recently digitized and are now available in the form of a raster. In GIS, each RAWS station was assigned a monthly PE value dictated by the grid that encompassed the station. The PE data, as mentioned earlier, was derived mostly from pan data thus the winter months are unreliable and often missing. The only months that contribute reliable data are from May-October period for the entire state.

In all three latitudinal transects the PE data show obvious trends of increasing PE with distance from the coast. The correlation coefficients are strong at 0.80, 0.91,

0.84 from May-October along the northern, central, and southern latitudinal transects, respectively (Figures 5.4, 5.5, 5.6). The PE transects show little variation between agroclimatic zones or past the 230 km distance from the coast, as with the ET_0 data set. Also of interest, the southern transect of PE did not exhibit any of the variability shown in the ET_0 dataset. Again, this is likely the result of sparse data in this region.

The longitudinal PE transects show very little change from south to north. The PE estimates decrease slightly from south to north along the western and central transects, but there is virtually no change across the eastern zone (Figures 5.7, 5.8, 5.9). The eastern zone could be flat because there were very few observations used for this region when the data set was created. This homogenous pattern contrasted the 50% decrease in seasonal ET_0 from the southern most RAWS to the northern most RAWS along the transect line.

Comparison Between Calculated ET_0 and Evaporation Pans

Comparison of the ASCE Penman-Monteith ET_0 quantities to Pan ET_0 shows the following, Wickiup, Medford, Corvallis, Malheur, Pendleton, and Summer Lake stations each show differences greater than 100 mm from May-October (Figure 5.12). The stations showing differences less than 100 mm are Willamette, Moro, Lookout Point, Hood River, Fern Ridge, and Madras. The stations with differences greater than 100 mm exist in the agroclimatic regions of South Central OR, Southwestern OR, Columbia Basin, Willamette Valley, Snake River Basin and represent a wide range of

elevations thus that illustrating large errors are possible across the entire state. It would seem that the lower elevation pans would yield the greatest errors because the RAWS network represents the higher elevation topography; however, this was not evident in the results. Table (5.1) shows the equation, interpolation, and error at each pan site for the period May-October.

Pan Station	Elev. (m)	Equation	Interp. Method	Error (mm)
N. Willamette	46	PM	IDW	-4.1
Moro	570	PM	Kriging	5.8
Corvallis State	70	HS	IDW	36.9
Hood River	155	PM	IDW	41.8
Wickiup Dam	1329	HS	IDW	-49.6
Fern Ridge Dam	146	HS	Kriging	-55.3
Summer Lake	1277	HS	IDW	60.7
Lookout Point	216	PM	IDW	-61.1
Madras	227	HS	Kriging	79
Malheur Branch	689	HS	Kriging	97.5
Medford	445	PM	Kriging	-100.5
Pendleton Branch	454	HS	Kriging	181.8

Table 5.1. Performance of equation versus evaporation pan converted to ET_0 including elevation and interpolation technique (IDW = inverse distance weighting).

Surprisingly, at seven of the pan sites the Hargreaves-Samani equation estimates of ET_0 were closer to the pan data, than the estimates from standardized ASCE Penman-Monteith equation. At Wickiup Dam, Corvallis State, and Summer Lake the Hargreaves-Samani equation, the use of the IDW interpolation technique showed the smallest error. Fern Ridge Dam, Malheur Branch, and Pendleton Branch each showed the least amount of error using the Hargreaves Samani as well, but the interpolation technique was Kriging for those stations. The ASCE Penman-Monteith equation outperformed the Hargreaves-Samani equation at Medford, N. Willamette, Hood River, Moro, and Lookout Point. Of those, only Moro and Medford used the

kriging interpolation technique. The differences between the four combinations, both equations and both interpolation techniques, were relatively small, which is probably why the results are so random.

Previous research has found that the Hargreaves-Samani equation performs poorly in windy regions and areas of high vapor pressure (Itenfisu et al. 2003). In another study by Hargreaves and Allen (2003), the Hargreaves-Samani equation was found to estimate 125% of measured ET from a lysimeter in humid environments and 91% in more arid climates. Evaporation pans are notorious for overestimating evaporation (ASCE-EWRI 2004). With the exception of Corvallis State, all of the stations where the Hargreaves-Samani estimates showed the least difference in humid regions were above the pans and below in the arid regions.

The coefficient used to convert pan evaporation to ET_0 , the interpolation procedure, and erroneous readings from the pan itself are potential sources that could cause inconsistencies in the data. The pan coefficient used to convert the data to ET_0 requires local monthly averages of wind, relative humidity, and land cover conditions surrounding the pan. Collecting this data was arduous, and a variety of sources were required to collect the necessary information. The ASCE-EWRI (2004) report also suggests further adjustments might be necessary based on reflection of solar radiation from shallow pans, where pans are enclosed by tall crops, windy or arid areas, painting schedules of the pan itself, the level at which the water is maintained in the pan, and whether or not a cage is protecting the pan from animal intrusions. Basically, each

pan requires some sort of local calibration to account for all of the possible influences. Such a calibration would be incredibly arduous and outside the realm of this project.

Completing the water balance equation

Before completing the water balance equation, ET_o needed to be converted to ET_a using the crop coefficient of 0.6 for evergreen land covers. The results are shown in Table 5.2.

(A)

Basin	Precip	Runoff	ET	PM IDW	PM Kri	Diff IDW	Diff Kri
qcco3	2420.2	2107.9	312.3	483.3	482.7	-0.66	-0.66
krbo3	1713.7	1124.3	589.4	641.9	632.5	-0.05	-0.04
tlmo3	3055.8	2490.2	565.6	408	401.3	0.38	0.39
lsto3	1063.3	831.7	231.6	564.0	577.2	-1.81	-1.88

(B)

Basin	Precip	Runoff	ET	HS IDW	HS Kri	Diff IDW	Diff Kri
qcco3	2420.2	2107.9	312.3	518.7	538.4	-0.80	-0.88
krbo3	1713.7	1124.3	589.4	675.7	602.2	-0.08	-0.01
tlmo3	3055.8	2490.2	565.6	455.1	476.6	0.26	0.21
lsto3	1063.3	831.7	231.6	577.3	551.6	-1.88	-1.74

Table 5.2. Comparison of ET_a from ASCE Penman-Monteith equation (A) and the Hargreaves-Samani equation (B) including coefficient adjustment and ET_a derived from a water balance equation. The last two columns were derived by subtracting the calculated ET_a from ET derived from the water balance equation using precipitation and runoff and then dividing by the area of the basin to normalize the results. Units are in mm. (qcco3 = Quartzville Creek, krbo3 = Illinois River near Kirby, OR, tlmo3 = Wilson River near Tillamook, OR, lsto3 = Lostine River)

In comparing the water balance derived ET and the ASCE Penman-Monteith ET_a , the differences for the smaller basins, qcco3 and lsto3, are large. The larger

basin, krbo3, shows the least normalized difference of -0.01 using the Hargreaves-Samani equation estimates and kriging interpolation. Again, it is surprising that the Hargreaves-Samani equation shows a smaller difference than the ASCE Penman-Monteith equation. In the qcco3 and lsto3 basins the normalized difference values of both equations are quite profound; however, the ASCE Penman-Monteith performed better than the Hargreaves-Samani. Erroneous streamflow, PRISM precipitation estimates, coefficient, interpolation, and ET_o estimates, and assumption of a closed basin are the six potential parties responsible for the difference in the results. Precipitation derived from PRISM modeling can have a bias of up to 4.5% annually (Daly et al. 1993). This error does not include error from the precipitation gages, which are the data source used to generate PRISM precipitation grids (Daly et al. 1993). Previous research indicates that precipitation gages consistently undercatch moisture (Legates and Willmott 1990) in areas susceptible to wind as a result of gage design. This would suggest, in the above water balance equation results, that ET_a from the ASCE Penman-Monteith could be accurate and the precipitation estimates are insufficient.

Streamflow data is determined in two steps. First, at a location along a river, a stage value is measured using an instrument. This stage value is then converted to streamflow (cubic feet per second) which is the result of a predetermined rating derived from a cross section of the river where volume per second is estimated. Ratings are required to be updated regularly due to environmental changes in the river channel. Data from sites where ratings are not updated regularly could be a source of

error in streamflow data. The crop coefficient for an evergreen land cover was derived from an irrigated environment and does not represent a water stressed forest. This could cause the coefficient to be insufficient; however, it would be assumed that a water stressed environment would incur more ET. Diversions and water losses are also a source of error in the water balance equation. The Lostine River receives diverted water from the Minam River for irrigation practices. Its possible that this additional water could have caused a larger runoff volume than what naturally would have occurred. In certain basins it is not feasible to assume a closed basin as water can be lost through percolation and ground water recharge. The effects of percolation and ground water recharge could be negligible when considering an annual scale.

Sensitivity of the ASCE Penman-Monteith

It is important to be able to quantify the impact of a bias in the data set from an invalid reading or error in the database. To accomplish that for this analysis, each data input was increased and decreased 10% of the range of annual variation for this analysis. The original ET_o value was then subtracted from the biased ET_o estimate. Inserting a bias in the maximum temperature (T_x and T_n) input showed the greatest effect throughout the calendar year (Figure 5.13). Temperature increases/decreases ranged from 0.5 to 0.88. The wind input shows a greater bias during June, July, August, September, and October. During other months, the difference is minimal. Showing differences less than 0.5 mm average daily value per month are solar radiation, minimum temperature, and dew point. From this analysis, it is evident that

biases in the maximum temperature and wind data during summer months would have the greatest effect on ET_o calculations.

The most pressure is put on managing water resources during the summer and early fall month. Because there is less available water during this time period dams, irrigation canals, and reservoirs have been developed to help the resource last. It is critical that these managers receive the best estimates of available water during this time. If there were a 10% positive bias in the t_x input into the ASCE Penman-Monteith equation for July, August and September, ET_o could be off by as much as 67 mm. Overestimating ET_o could cause more water to be distributed than necessary. On the opposite side of the spectrum, if there were a negative 10% bias in the recorded maximum temperature, then during the months of June, July, and August, ET_o could be underestimated by 68 mm. Underestimating the atmosphere's demand for moisture could result in too little water allotted for filling a reservoir or distributing water into the drier months of later summer and early fall in Oregon.

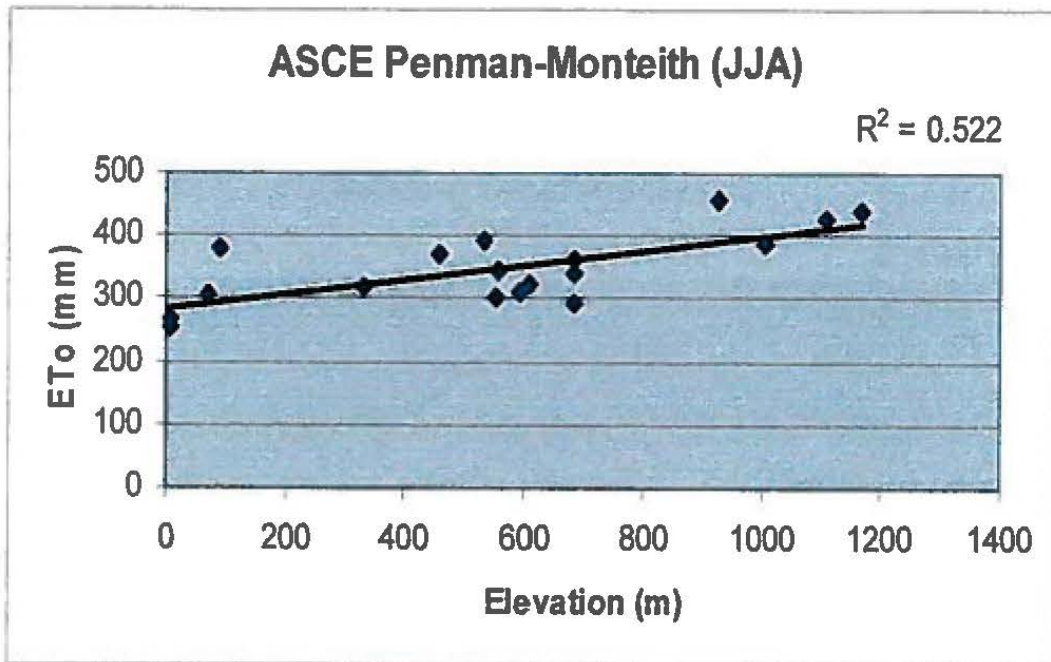
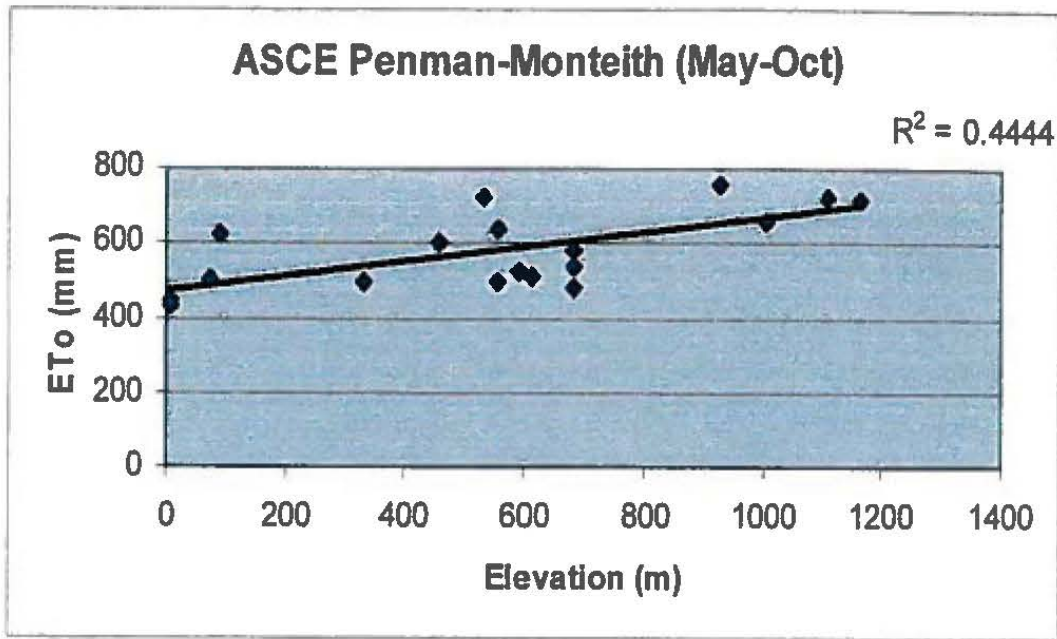


Figure 5.1. ASCE Penman-Monteith ETo value totals for Coastal Region JJA vs. elevation (below), may-oct (above) vs. elevation.

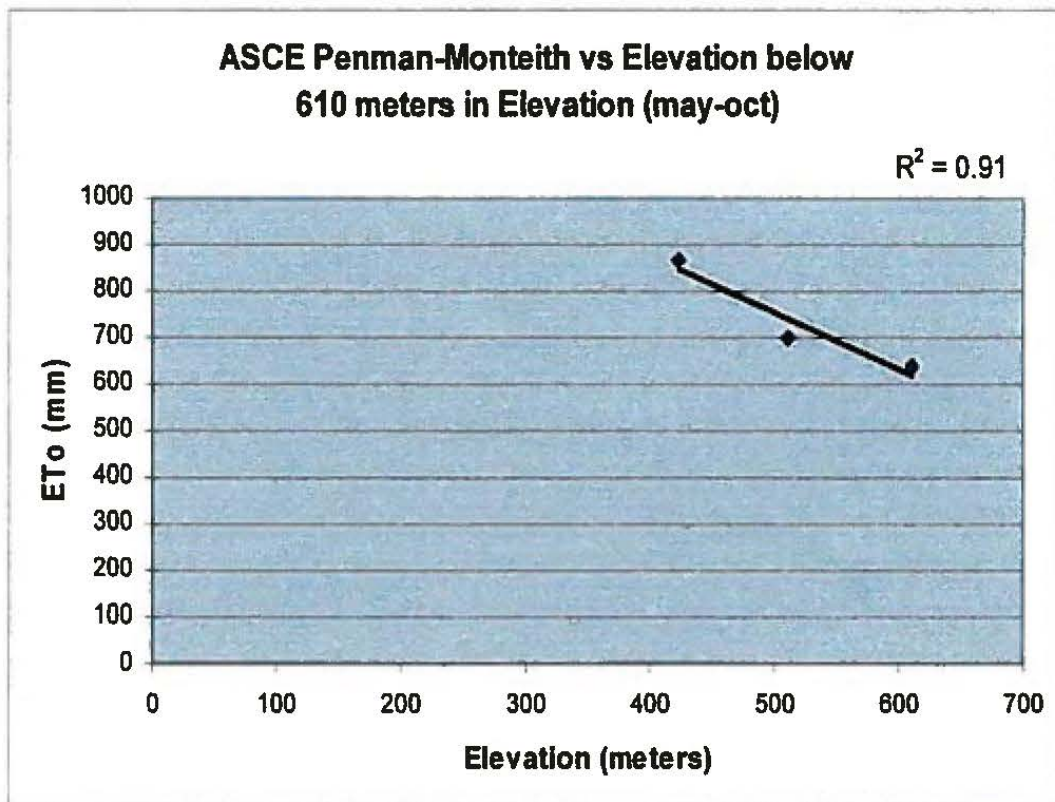
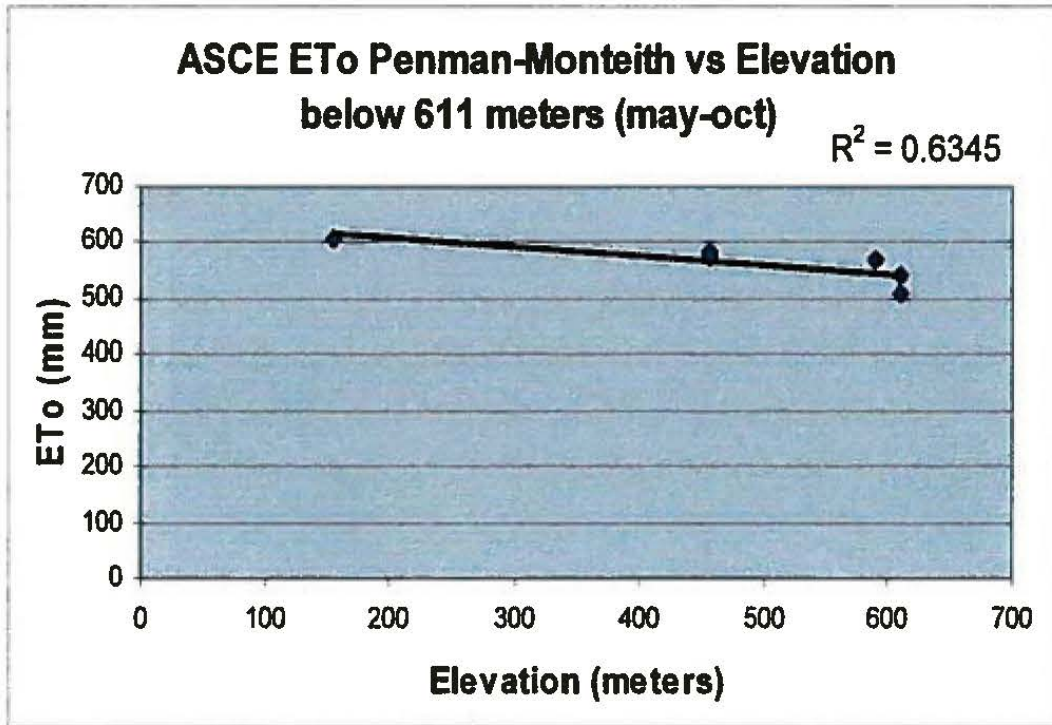


Figure 5.2. Reduction in ET_0 with regard to elevation below 611 meters in Willamette Valley (above) and Southwestern Oregon (below) regions.

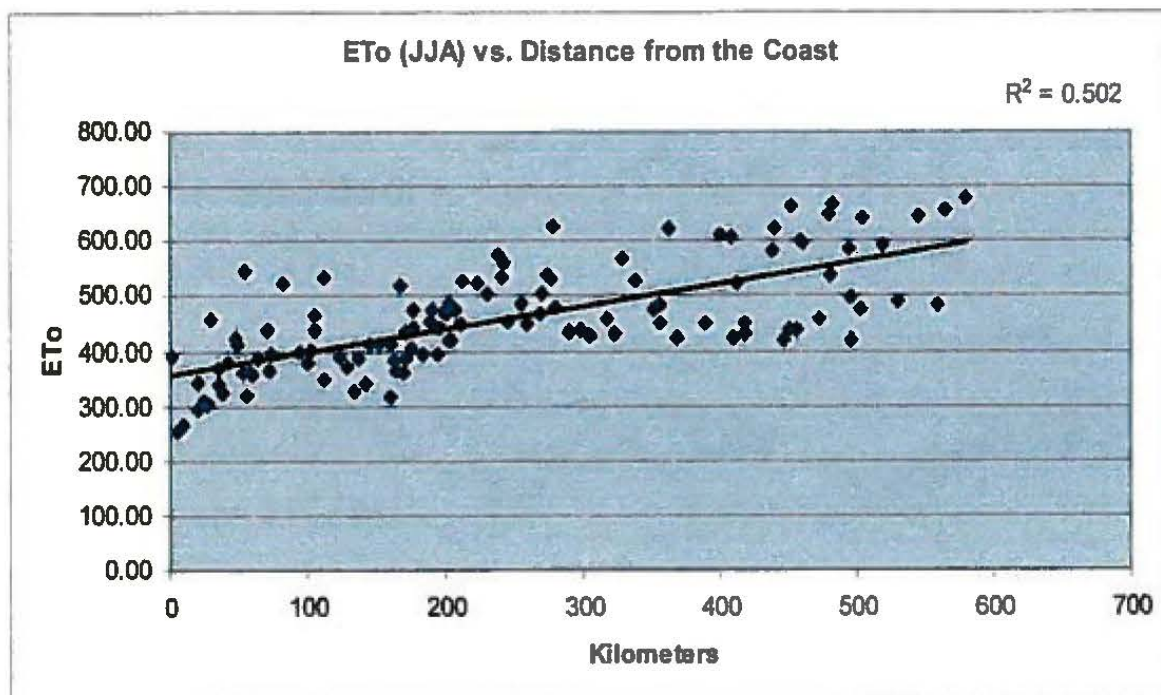


Figure 5.3. ASCE Penman-Monteith ETo vs. distance from the Pacific Ocean

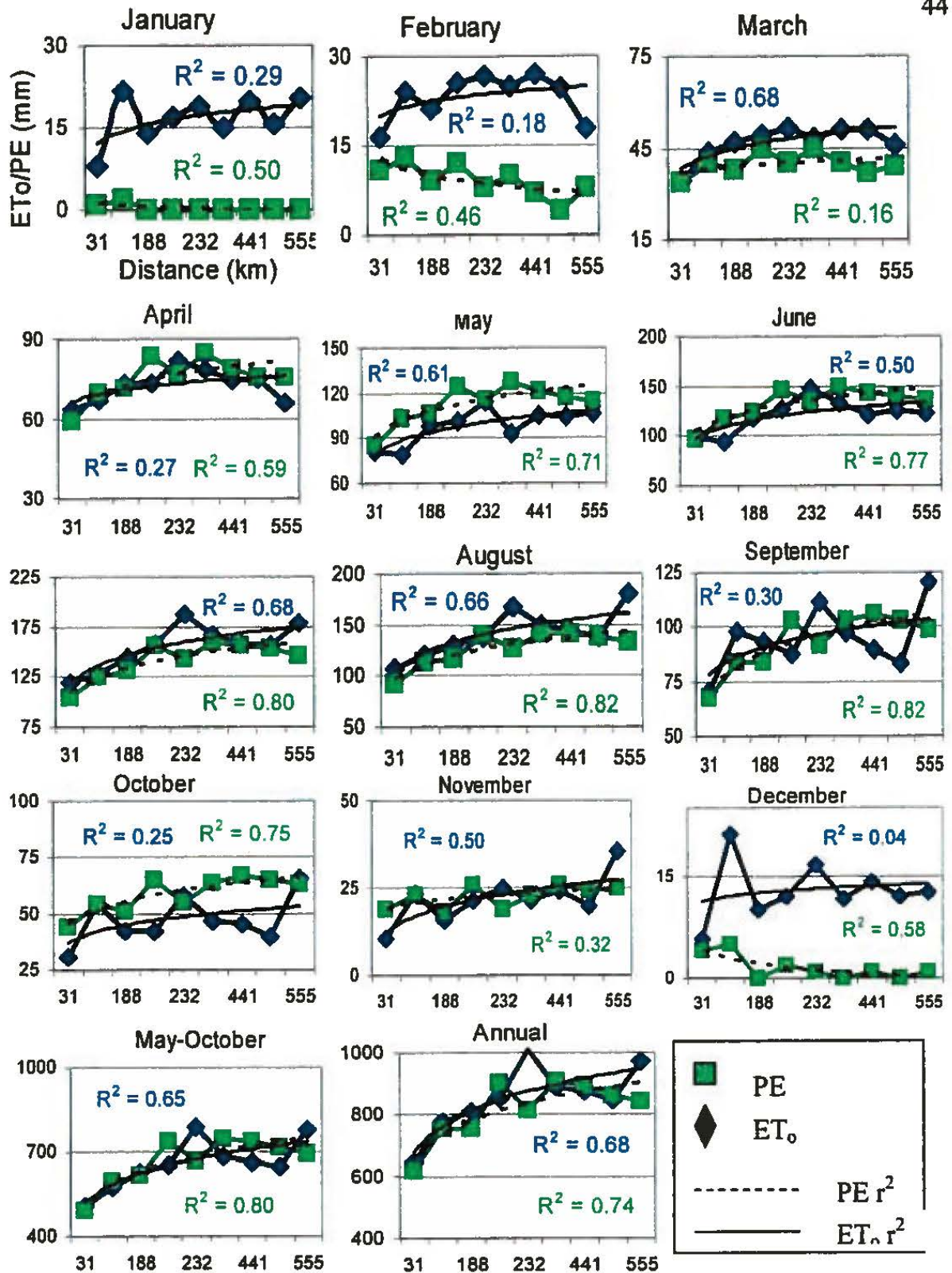


Figure 5.4. Northern latitudinal transects across Oregon. The transect portrays the change in ET₀ and PE with regard to distance from the Pacific Ocean.

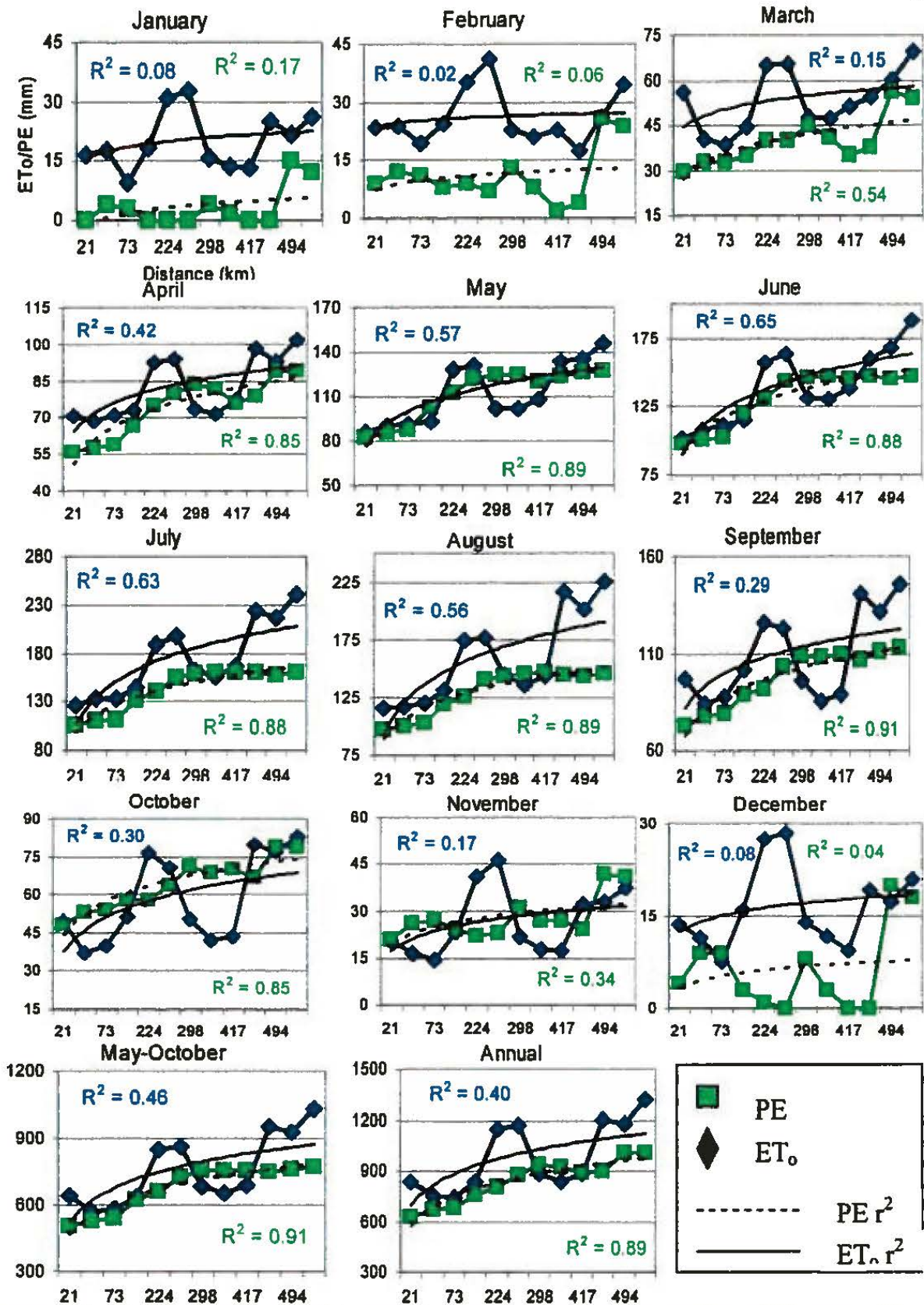


Figure 5.5. Central latitudinal transect representing a cross section of Oregon. The transect portrays the change in ET₀ and PE with regard to distance from the Pacific Ocean.

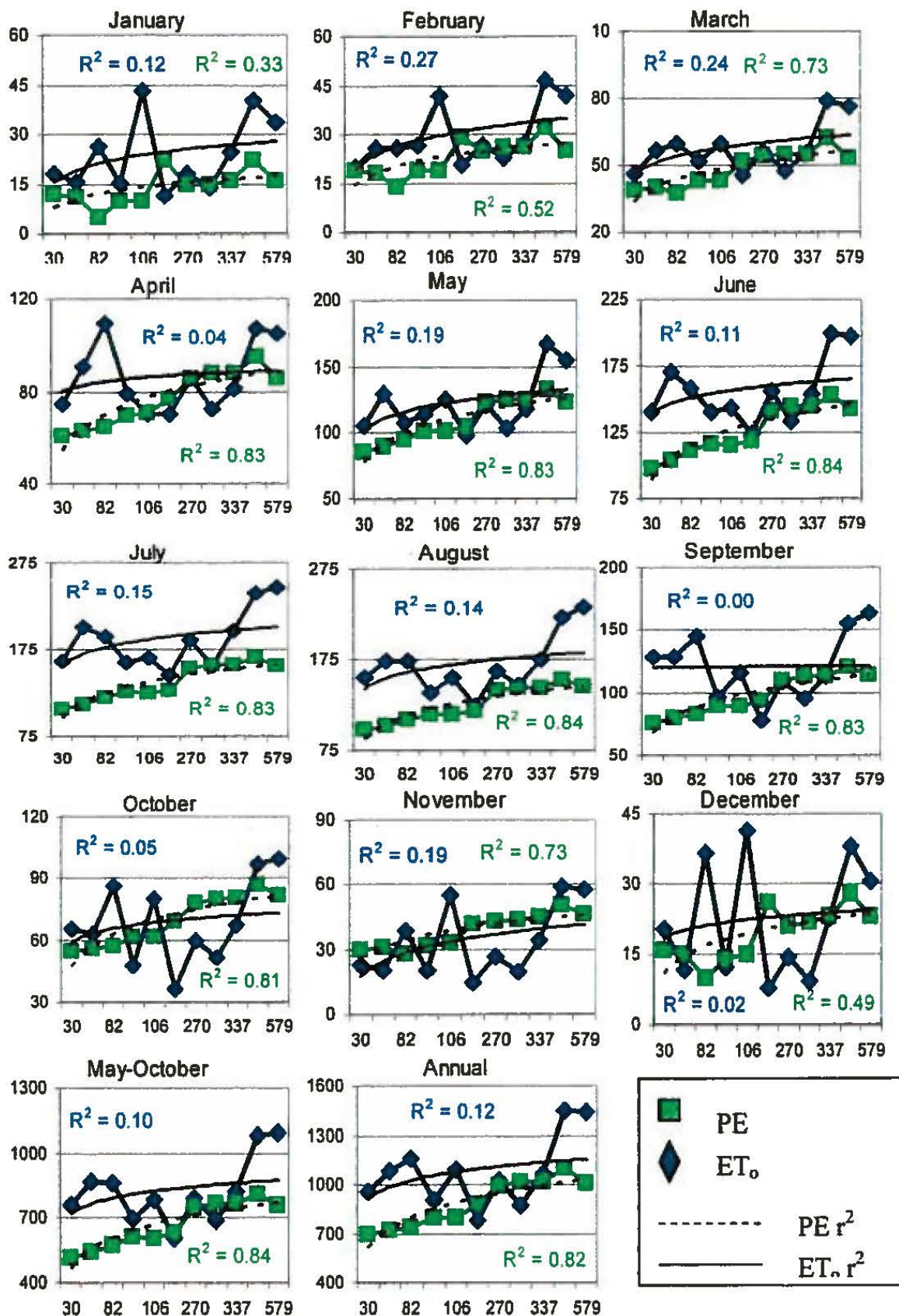


Figure 5.6. Southern latitudinal transect representing a cross section of Oregon. The transect portrays the change in ET_0 and PE with regard to distance from the Pacific Ocean.

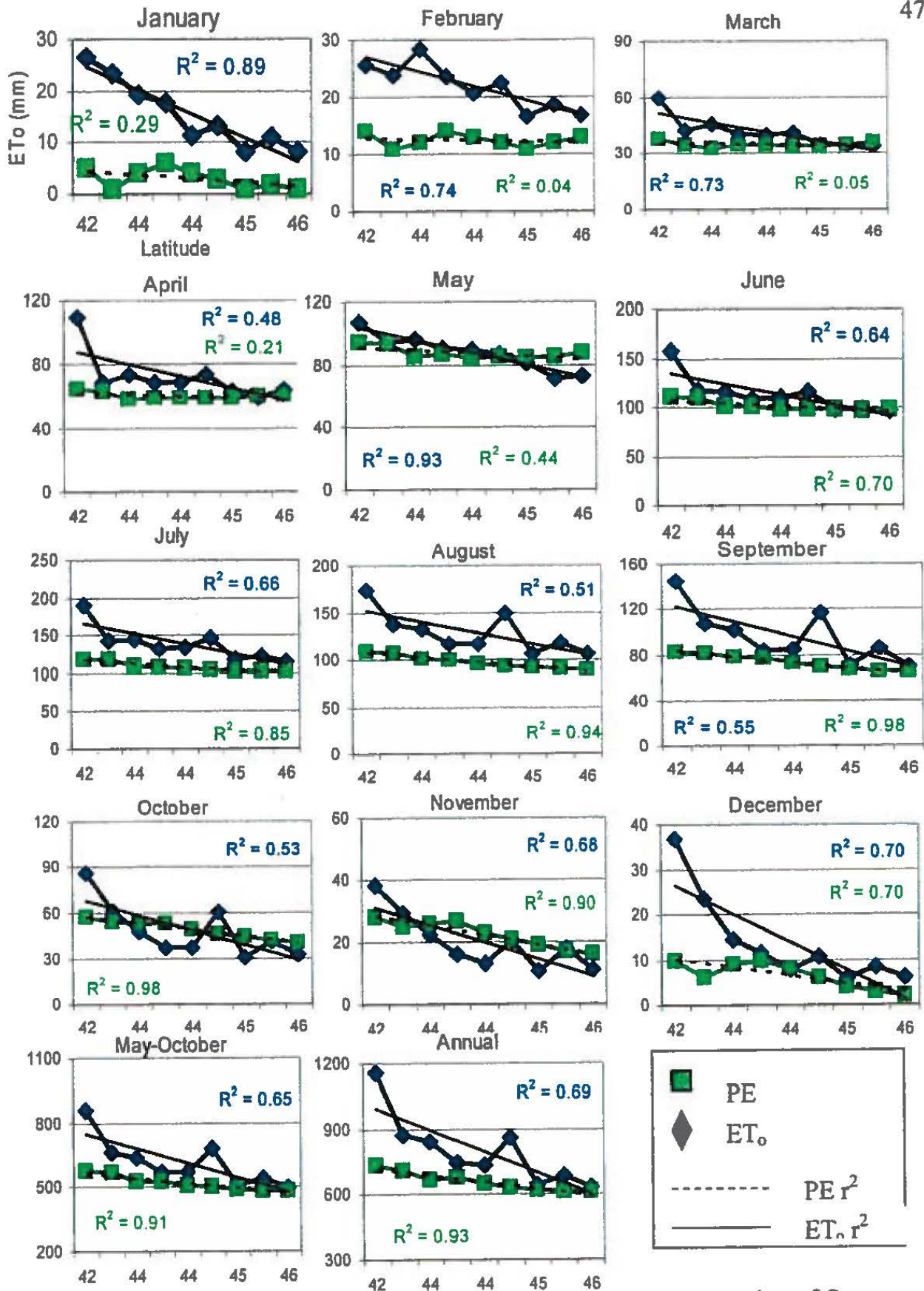


Figure 5.7. Western longitudinal transects representing a cross section of Oregon that compares the spatial characteristics of each data set with regard to latitude

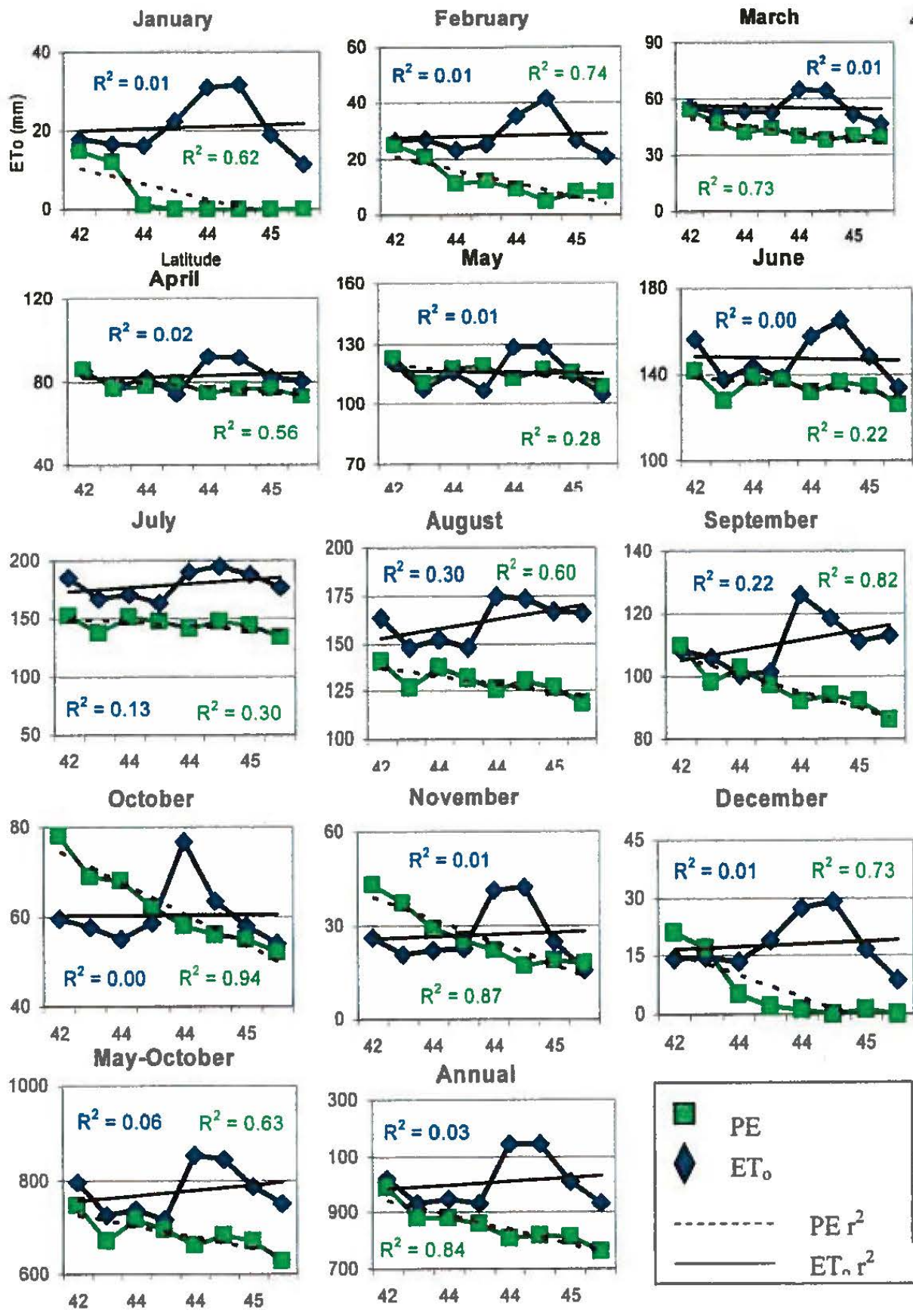


Figure 5.8. Central longitudinal transects representing a cross section of Oregon that compares the spatial characteristics of each data set with regard to latitude.

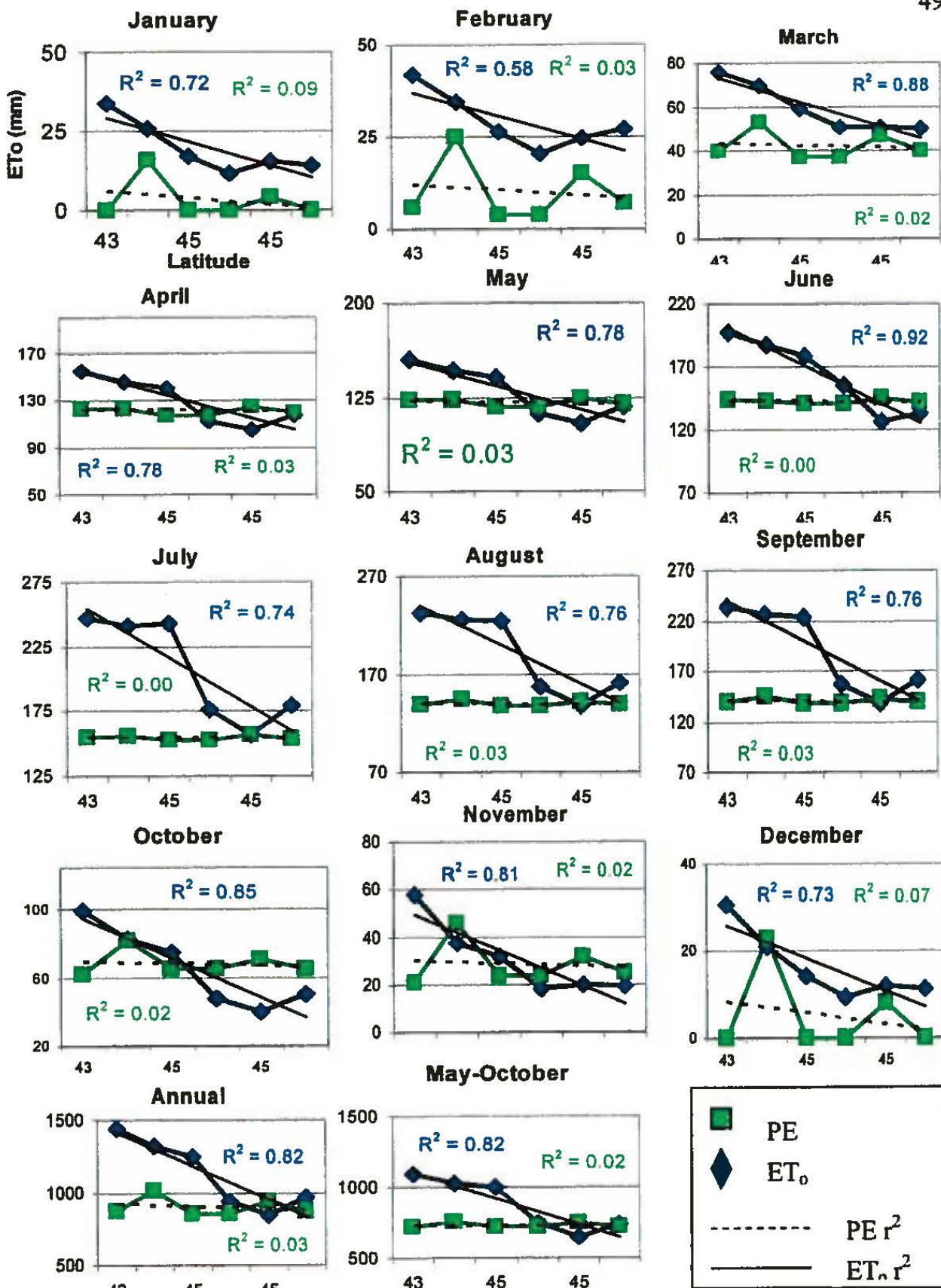


Figure 5.9. Eastern longitudinal transects representing a cross section of Oregon that compares the spatial characteristics of each data set with regard to latitude.

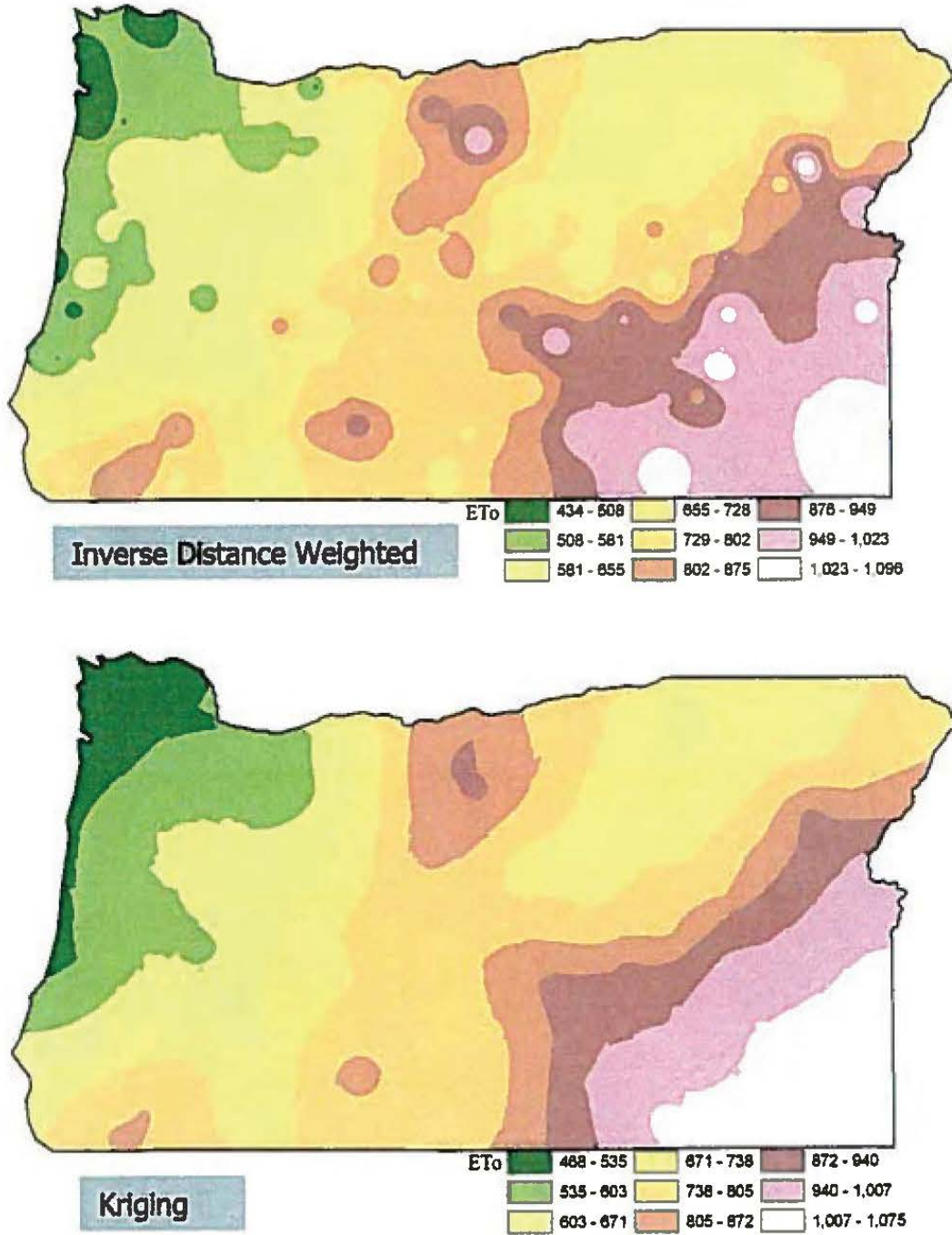


Figure 5.10. ASCE Penman-Monteith derived ET_0 point values interpolated into grids using the Inverse Distance Weighted (above) and Kriging (below) techniques.

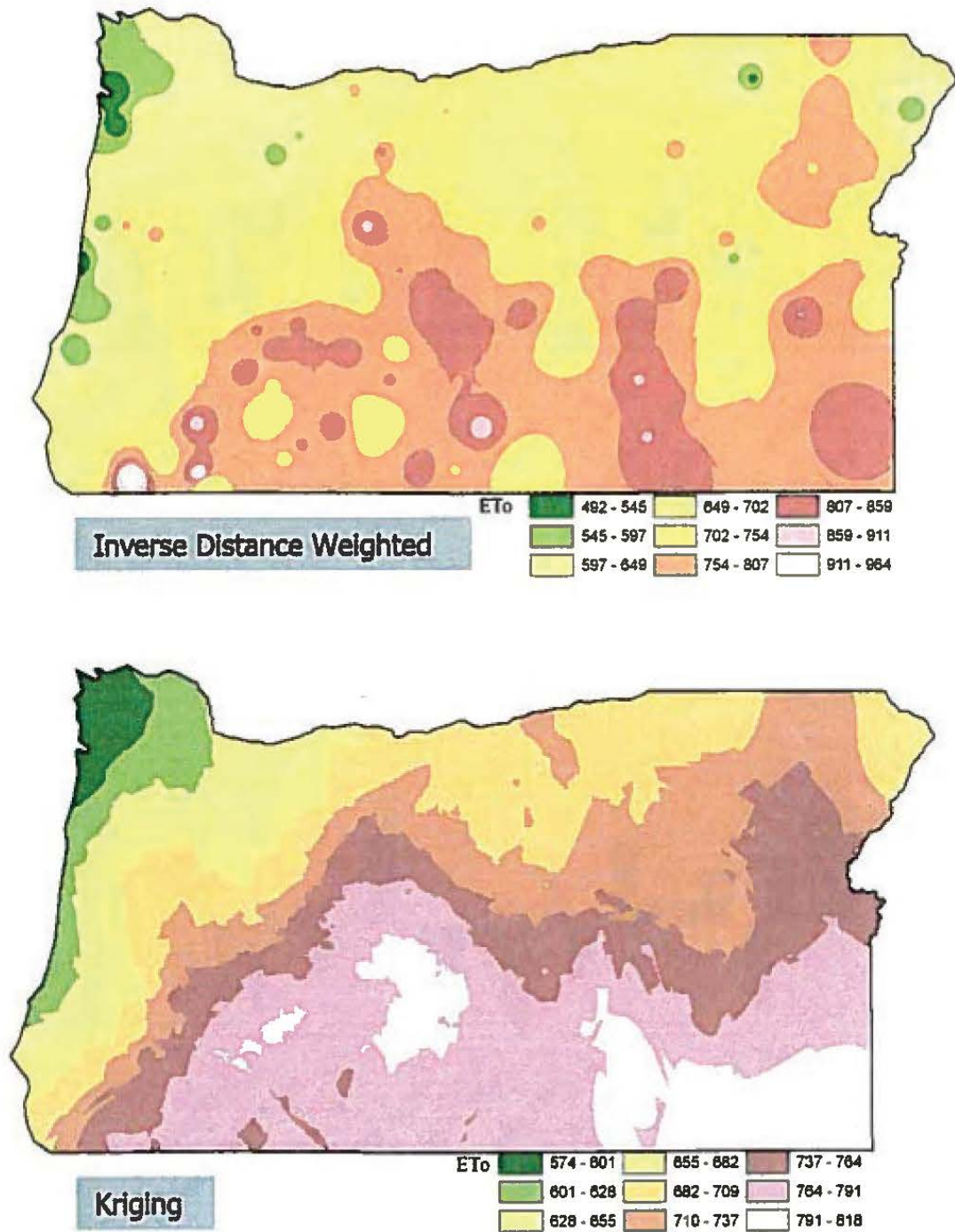


Figure 5.11. Hargreaves-Samani derived ET_0 point values interpolated into grids using the Inverse Distance Weighted (above) and Kriging (below) techniques.

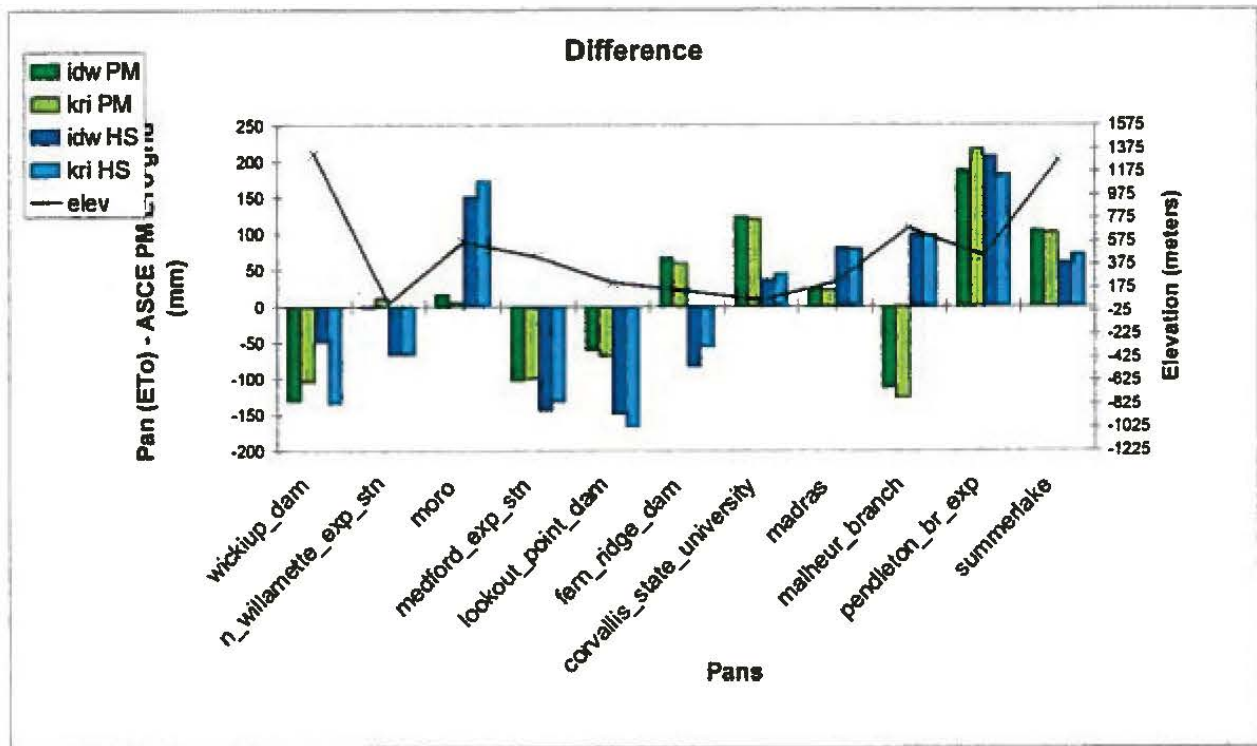
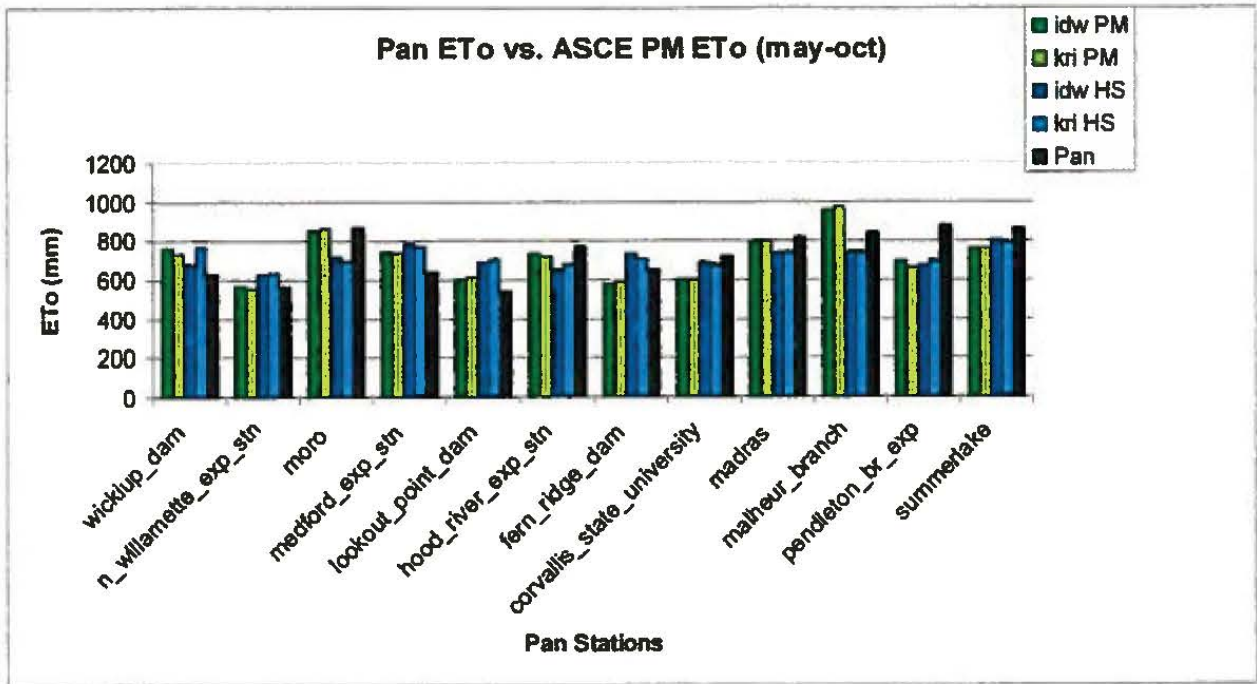


Figure 5.12. Comparison of ETo using NWS Class A evaporation pans. The Pan ETo vs. ASCE PM ETo (may-oct) graph compares the average May-October quantity of ETo from 1998-2002. The chart, Difference, represents the difference between the pans and the ETo estimate (pans – ETo) and the elevation of the pans.

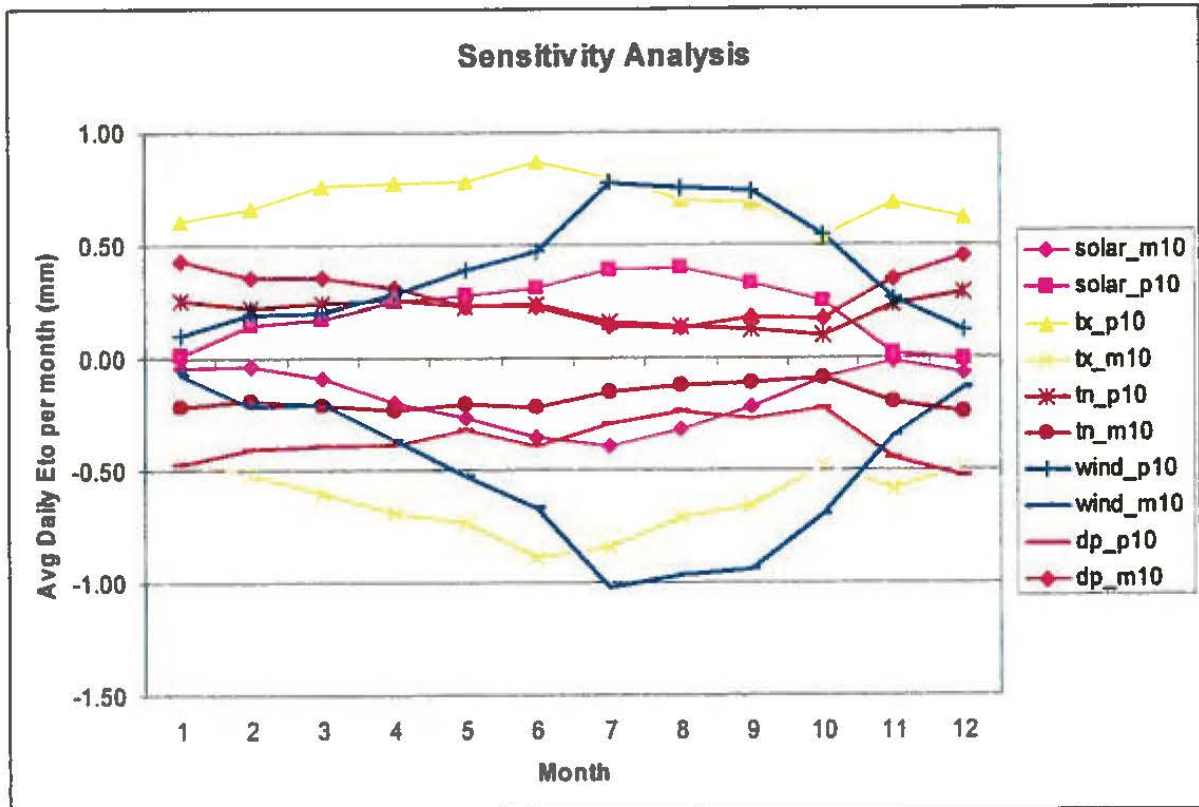


Figure 5.13. Sensitivity analysis of ASCE Penman-Monteith Equation. Solar radiation, temperature, wind, and dew point are individually increased and decreased 10% of the each elements annual fluctuation to isolate the impact. The RAWS Lava Butte, during calendar year 2002 was chosen for the analysis. Regarding the labels, “p10” means plus 10% and “m10” means minus 10%.

SUMMARY AND PROPOSED RESEARCH

In this study I analyzed difference between the PE data set derived in 1982 and the modern ASCE Penman-Monteith derived ET_0 . This study also tested the results of the ASCE Penman-Monteith data set against directly measured evaporation pans and in a water balance equation to forecast its usefulness in basin calibrations conducted for streamflow modeling.

This study compared the spatial variation of PE and ET_0 to determine whether or not the PE data set used operationally at the NWRFC portrays characteristics evident in ASCE Penman-Monteith derived ET_0 . The first conclusion was that there is no apparent relationship between ET_0 and increasing elevation in the agroclimatic sub regions of Oregon. Perhaps there is a relationship below 611 meters, but the limited number of stations in each region below this elevation requires further investigation. These results are contrary to the results from the Farnsworth et al. (1982) study in which it was found that PE decreases with elevation in both California and New Mexico (Farnsworth et al. 1982). It is possible that the more mathematically robust ASCE Penman-Monteith equation better captures what is naturally occurring. One of the elements that increase ET_0 estimates and increases with elevation is solar radiation. In the study by Farnsworth et al. (1982) the solar radiation input may not have properly represented the higher elevations.

The next conclusion was found by dissecting Oregon with transect lines oriented both in latitudinal and longitudinal directions. From the latitudinal transects

it was found that in the northern portion of the state, ET_0 increases with distance from the Pacific Ocean up to approximately 230 km, or just on the other side of the Cascade Crest. The PE data set follows a similar pattern, with the variability occurring at approximately 200 km, or 30 km closer to the coast than the ET_0 data set. In Central Oregon, the PE data set showed a steady increasing trend up to approximately 300 km before leveling. The ET_0 data set showed more variability near the coast, just east of the Cascade Crest and again in Eastern Oregon, suggesting that the PE data set does not capture the variability caused by the topography in central Oregon. The two data sets also did not agree along the southern transect. The PE data set showed a steady rise 280 km inland before leveling out. The ET_0 transect showed substantial variation crossing the coastal, Southwestern Oregon, South central Oregon, and Snake agroclimatic regions.

Differences were also noted between the two data sets along the longitudinal transects. Interestingly enough, the winter months show the strongest correlations in this analysis. Along the western transect, PE and ET_0 show very similar trends suggesting the two data sets are in agreement over the spatial variation in this region. The central longitudinal transects do not show similar patterns. The PE data set shows a steady decreasing trend in PE to the north while ET_0 shows erratic variability. The ET_0 data set suggests that toward the transition between the northern portion of the South Central and the Columbia Basin agroclimatic region ET_0 rates begin increasing. In the eastern region of Oregon, the PE data along the transect indicates that the rate is

virtually constant while ET_o shows a strong decreasing trend, where ET_o decreases nearly 50% in the May-October resolution from south to north.

Verifying the ET_o calculations against the evaporation pans was done to verify the results of the calculations. There appeared to be no advantage to using either the standardized ASCE Penman-Monteith Equation or the Hargreaves-Samani equation. There also appeared to be no advantage to using either the IDW or kriging as a means of interpolating data. The effectiveness of each method proved to be random in this analysis.

In the results from the water balance application, in one basin the Hargreaves-Samani outperformed the ASCE Penman-Monteith equation. In the two smaller basins, where both estimates appeared to be off, the ASCE Penman-Monteith estimates were closer to the ET_a derived from the water balance equation. In this small sample of four basins, there was no strong indication that one equation would consistently out perform the other. The Kriging interpolation method did prove to be more accurate.

The results from this study indicate there is still an enormous gap in evapotranspiration research. Mostly, studies verifying the relationship between ASCE Penman-Monteith ET_o and water stressed vegetative characteristics are in demand. Field studies need to be designed where evapotranspiration of a wide variety of land covers are observed. In agricultural areas, there is ample research documenting these characteristics during the growing seasons. However, in non-agricultural regions, there is a void of this information.

REFERENCES:

- Allen, Richard G., M.E. Jensen, J.L. Wright, and R.D. Burman. 1989. Operational estimates of reference evapotranspiration. *Agronomy Journal*. 81 (4): 650-662.
- Allen, Richard G., L.S. Pereira, D. Raes, M. Smith. 1998. Crop evapotranspiration: Guidelines for computing crop water requirements. FAO Irrigation and Drainage paper 56.
- Anderson, Eric. 2002. *Calibration of Conceptual Hydrologic Models for Use in River Forecasting*. Instructional Document: Hydrologic Research Laboratory, NWS.
- ASCE-EWRI. 2004. *The ASCE Standardized Reference Evapotranspiration Equation*. Technical Committee report to the Environmental and Water Resources Institute of the American Society of Civil Engineers from the Task Committee on Standardization of Reference Evapotranspiration. 173 p.
- Beebee, Robin A and Michael Manga. 2004. Variation in the relationship between snowmelt runoff in Oregon and ENSO and PDO. *Journal of the American Water Resources Association*. August. 1011-1024.
- Daly, Christopher, Ronald P. Neilson, Donald L. Phillips. 1993. A statistical-topographic model for mapping climatological precipitation over mountainous terrain. *Journal of Applied Meteorology*. 33: 140-158.
- Duffie, J.A., and W.A. Beckman. 1980. *Solar Engineering of Thermal Processes*. Wiley, New York. p. 1-109.
- Farnsworth, Richard K., E.S. Thompson, E.L. Peck. 1982. Evaporation atlas for the contiguous 48 United States. *NOAA Technical Report NWS 33*. June: 1-26
- Farnsworth, Richard K., and Edwin S. Thompson. 1982. Mean monthly, seasonal, and annual pan evaporation for the United States. *NOAA Technical Report NWS 34*. December: 1-82.
- Frei, Allan, R.L. Armstrong, M.P. Clark, M.C. Serreze. Catskill mountain water resources: vulnerability, hydroclimatology, and climate-change sensitivity. *Annals of the Association of American Geographers*. 2: 203-224.
- Grismer, M.E., M. Orang, R. Snyder, R. Maytac. 2002. Pan evaporation to reference evapotranspiration conversion methods. *Journal of Irrigation and Drainage Engineering*. May/June: 180-184.

- Hargreaves, George H. and Richard G. Allen. 2003. History and evaluation of Hargreaves evapotranspiration equation. *Journal of Irrigation and Drainage Engineering*. January/February: 53-63.
- Itenfisu, Daniel, R.L. Elliot, R.G. Allen, I.A. Walter. 2003. Comparison of Reference Evapotranspiration Calculations as Part of the ASCE Standardization Effort. *Journal of Irrigation and Drainage Engineering*. Vol 129, 6:440-448.
- Kagan, J., S. Caicoo. 1996. Manual of Oregon Actual Vegetation, Oregon Gap Analysis Program. U.S. Fish and Wildlife Service, Portland, OR.
- Legates, D.R., and C.J. Willmott. 1990: Mean seasonal and spatial variability in gauge-corrected, global precipitation. *International Journal of Climatology*, vol. 10, 111-127.
- Lindsey, Scott D., and Richard K. Farnsworth. 1997. Sources of solar radiation estimates and their effect on daily potential evaporation for use in streamflow modeling. *Journal of Hydrology*. 201: 348-366.
- Linsley, Ray K., M.A. Kohler, J.L., H. Paulhus. 1982. *Hydrology for Engineers*. Third Edition. McGraw-Hill Inc. pp 25-26, 31-32.
- Lu, Jianbiao, G. Sun, S.G. McNulty, D.M. Amatya. 2003. Modeling actual evapotranspiration from forested watersheds across the southeastern United States. *Journal of the American Water Resources Association*. August: 887-896.
- Martinez-Cob, A., and Richard H. Cuenca. 1992. Influence of elevation on regional evapotranspiration using multivariate geostatistics for various climatic regimes in Oregon. *Journal of Hydrology*. 136: 353-380.
- Monteith, J.L. 1965. Evaporation and the Environment. *Water in the Planet*. 205-234.
- Schreiner, Anthony J., D. A. Unger, W.P. Menzel, G.P. Ellrod, K.I. Strabella, J.L. Pellet. 1993. A Comparison of Ground and Satellite Observations of Cloud Cover. *Bulletin of American Meteorological Society*. 74 (10) 1851-1861
- Penman, H.L. 1948. Natural evaporation from open water, bare soil, and grass. *Natural Evaporation*. 120-145.
- Redmond, K.T. 1985. An inventory of climate data for the state of Oregon. Climate Research Institute, Oregon State University, Corvallis, Report SCP-3, pp. 160.
- Snyder, R.L., M. Orang, S. Maytac, S. Sching. Crop Coefficients. UC Davis Department of Biometeorology. 2002. <http://biomet.ucdavis.edu/evapotranspiration> (last accessed May 10, 2006).

USGS. 2006. waterdata.usgs.gov/or/nwis/current?submitted_form=introduction. (last accessed May 23, 2006).

Vignola, Frank, and Richard Perez. 2004. Solar Resource GIS Data base of the Pacific Northwest using Satellite Data. Unpublished Final Report. pp. 73.

Western Region Climate Center. 2006. Average Annual Precipitation in Oregon <http://www.wrcc.dri.edu/pcpn/or.gif> (last accessed May 31, 2006).

APPENDIX A: ASCE PENMAN-MONTEITH EQUATION

The below equations are from Snyder et al. (2002).

The first step is to calculate extraterrestrial radiation (R_a), which will then be used for calculating net radiation (R_n). The equation is from Duffie and Beckman (1980).

Eqn 2.1 R_a = extraterrestrial radiation ($\text{MJ m}^{-2} \text{ d}^{-1}$)

$$R_a = \frac{(24 * 60)G_{sc}d_r [\omega_s \sin\delta \sin\phi + \cos\phi \sin\delta \sin\omega_s]}{\pi}$$

$$G_{sc} = \text{solar constant in MJ m}^{-2} \text{ min}^{-1}$$

$$G_{sc} = 0.082$$

$$\sigma = \text{Steffan-Boltzman constant in MJ m}^{-2} \text{ d}^{-1} \text{ K}^{-4}$$

$$\sigma = 4.90 \times 10^{-9}$$

ϕ = latitude in radians converted from latitude (L) in degrees

$$\phi = \frac{\pi L}{180}$$

d_r = correction for eccentricity of Earth's orbit around the sun on day i of the year

$$d_r = 1 + 0.033 \cos\left(\frac{2\pi * i}{365}\right)$$

δ = declination of the sun above the celestial equator in radians on day i of the year

$$\delta = 0.409 \sin\left(\frac{2\pi * i}{365} - 1.39\right)$$

ω_s = sunrise hour angle in radians

$$\omega_s = \cos^{-1} [-\tan\phi \tan\delta]$$

The next step is to calculate R_n expected over grass in $\text{MJ}/(\text{m}^2 \text{d}^1)$ using equations from Allen et al. (1994). Calculations for radiation in such an environment will follow the below steps:

$$\text{Eqn 2.2. } R_n = R_{ns} + R_{nl} \text{ (where } R_n \text{ is in } \text{MJ}/(\text{m}^2 \text{d}^1)\text{)}$$

R_{so} = clear sky total global solar radiation at the Earth's surface in $\text{MJ}/(\text{m}^2 \text{d}^1)$

$$R_{so} = R_a (0.75 + 2.0 * 10^{-5} E_i)$$

R_{ns} = net solar radiation over grass as a function of measured solar radiation (R_s) in $\text{MJ}/(\text{m}^2 \text{d}^1)$

$$R_{ns} = (1 - 0.23) R_s$$

f = a cloudiness function of R_s and R_{so}

$$f = 1.35 \left(\frac{R_s}{R_{so}} \right) - 0.35$$

$e_s(T_x)$ = saturation vapor pressure (kPa) at the maximum daily air temperature (T_x) in $^{\circ}\text{C}$

$$e_s(T_x) = 0.6108 \exp \left(\frac{17.27 T_x}{T_x + 237.3} \right)$$

$e_s(T_n)$ = saturation vapor pressure (kPa) at the minimum daily air temperature (T_n) in $^{\circ}\text{C}$

$$e_s(T_n) = 0.6108 \exp \left(\frac{17.27 T_n}{T_n + 237.3} \right)$$

e_a = actual vapor pressure or saturation vapor pressure (kPa) at the mean dew point temperature from the daily maximum (T_x) and minimum (T_n) temperature ($^{\circ}\text{C}$) and maximum (RH_x) and minimum (RH_n) relative humidity (%).

$$e_a = \frac{((\text{RH}_x + \text{RH}_n)/2)}{(((50/(e_s * T_x)) + ((50/(e_s * T_n))))}$$

e_a = actual vapor pressure or saturation vapor pressure (kPa) at the daily mean dew point (T_d) temperature.

$$e_a = 0.6108 \exp \frac{(17.27T_d)}{(T_d + 237.3)}$$

ϵ' = apparent 'net' clear sky emissivity
 $\epsilon' = 0.34 - 0.14 \sqrt{e_a}$

$$R_{nl} = \text{net long wave radiation in MJ m}^{-2} \text{ d}^{-1}$$

$$R_{nl} = -f \epsilon' \sigma * \frac{(T_x + 273.15)^4 + (T_n + 273.15)^4}{2}$$

The next calculations derive physical elements not measured at RAWS but persist in natural environments.

(2.3) β = barometric pressure in kPa as a function of elevation (E_l) in meters

$$\beta = 101.3 \left(\frac{293 - 0.0065 E_l}{293} \right)^{5.26}$$

(2.4) λ = latent heat of vaporization in (MJ kg^{-1})
 $\lambda = 2.45$

(2.5) γ = psychrometric constant in $\text{kPa } ^{\circ}\text{C}^{-1}$
 $\gamma = 0.00163 \frac{\beta}{\lambda}$

(2.6) T_m = mean daily temperature in $^{\circ}\text{C}$

$$T_m = \frac{T_x + T_n}{2}$$

(2.7) e^o = saturation vapor pressure at T_m

$$e^o = 0.0016108 \exp \left(\frac{17.27 * T_m}{T_m + 237.3} \right)$$

(2.8) Δ = slope of the saturation vapor pressure curve ($\text{kPa } ^{\circ}\text{C}^{-1}$) at mean air temperature (T_m)

$$\Delta = \frac{4099 e^o}{(T_m + 237.3)^2}$$

(2.9) G = soil heat flux density in $\text{MJ m}^{-2} \text{d}^{-1}$
 $G \approx 0$

(2.10) e_s = mean daily saturation vapor pressure (kPa)

$$e_s = \frac{e_s(T_x) + e_s(T_n)}{2}$$